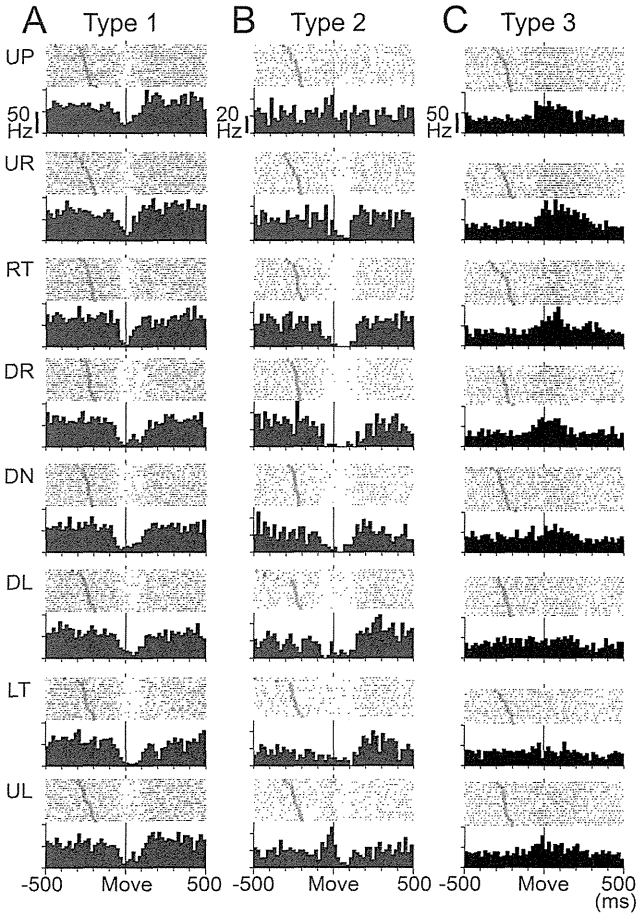


**Figure 4. Three types of SS activity in wrist-movement-related PCs.** Raster plots and histograms of SS activity for typical examples of three types of SS activity in PCs with RFs in the distal part of the arm (see Materials and Methods). SS activity recorded in the pronated posture is illustrated. PCs were classified into three types based on movement-related modulations between −200 to +200 ms relative to movement onset. All plots are aligned on movement onset (Move), indicated by the solid line in the center of each plot. In addition, all rasters are sorted by the timing of Go cue (indicated by filled gray triangles). Histogram bin width = 20 ms. A: SS activity of type 1 PCs showed suppression before movement onset. Note that the depth and duration of suppression varied with movement direction. B: SS activity of type 2 PCs showed suppression before movement onset for some directions and facilitation for other directions. C: SS activity of type 3 PCs showed facilitation before movement onset. Note that the amplitude and duration of the facilitation varied with movement direction. Note also that the scale bars for discharge rate shown in the top row of panels differ for the three cells. UP: up, UR: upper right, RT: right, DR: down right, DN: down, DL: down left, LT: left, UL: upper left. In the pronated posture, UP, DN, LF and RT correspond to extension, flexion, radial deviation and ulnar deviation of the wrist joint, respectively.
doi:10.1371/journal.pone.0108774.g004

discharge rate around movement onset (−200 to +300 ms relative to the onset of movement) to the spontaneous activity level using Student's *t*-test (significance set at $p<0.01$) for movements in each direction and posture. We classified cells that exhibited significant differences in discharge rate for any direction and in any posture as movement-related. The movement-related activity of those cells is the focus of this report. For each movement-related cell, we used a bootstrapping method to identify whether the cell was directionally tuned ($p<0.05$) [34].

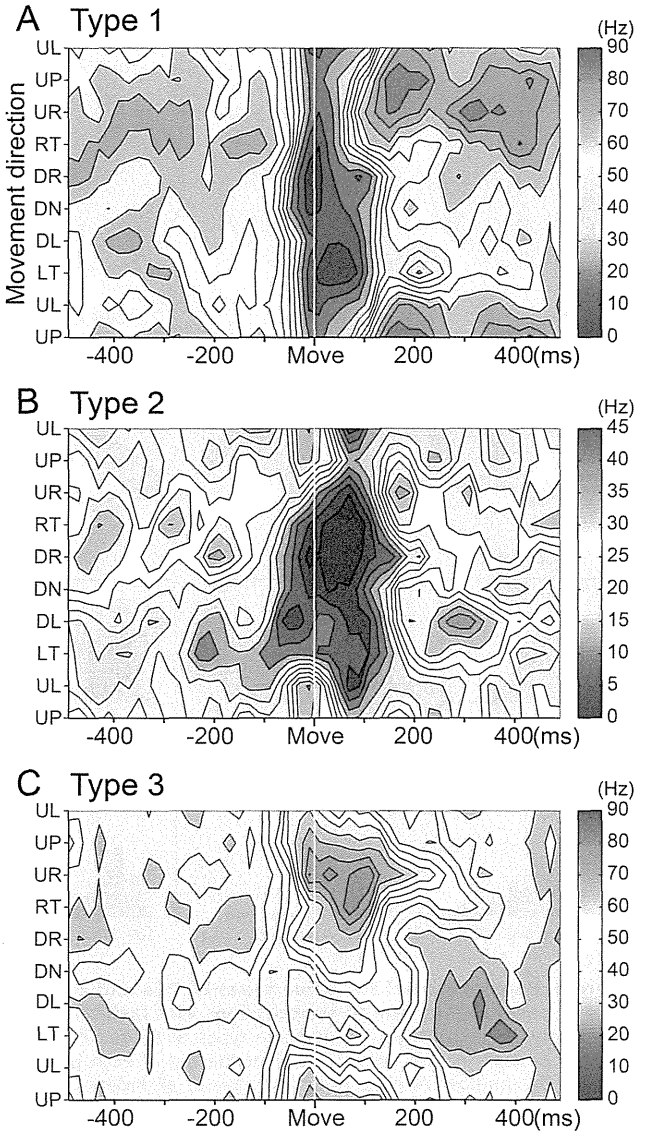


**Figure 5. Contour plots of three types of SS activity.** Spatiotemporal maps of SS activity of type 1 (A), type 2 (B) and type 3 (C) PCs in relation to 8 movement directions (the same material illustrated in Figure 4). These plots were generated with MATLAB. Color code was adjusted according to the maximum firing rate in each PC.
doi:10.1371/journal.pone.0108774.g005

## Calculation of onset of movement-related modulations for PCs and DN cells and display of neural activity as pseudo-colored maps

To analyze the activity of the wrist-movement-related PCs and DN cells, we processed the activity of each cell as follows. For movements in each direction and posture, we plotted a histogram of neuron activity in 20 ms bins. To display spatio-temporal patterns of activity for individual PCs and DN cells, we made pseudo-colored contour plots of the histogram. For each cell, the histograms for eight directions of movement were smoothed with a Savitzky-Golay filter (polynomial order: 3, frame size: 7), and a contour plot was generated using a standard function provided by MATLAB. In addition, to display the population activity for all movement-related PCs or DN cells in each movement direction and posture, we made pseudo-colored maps of the histograms of all PCs or DN cells according to the following procedure. First, we

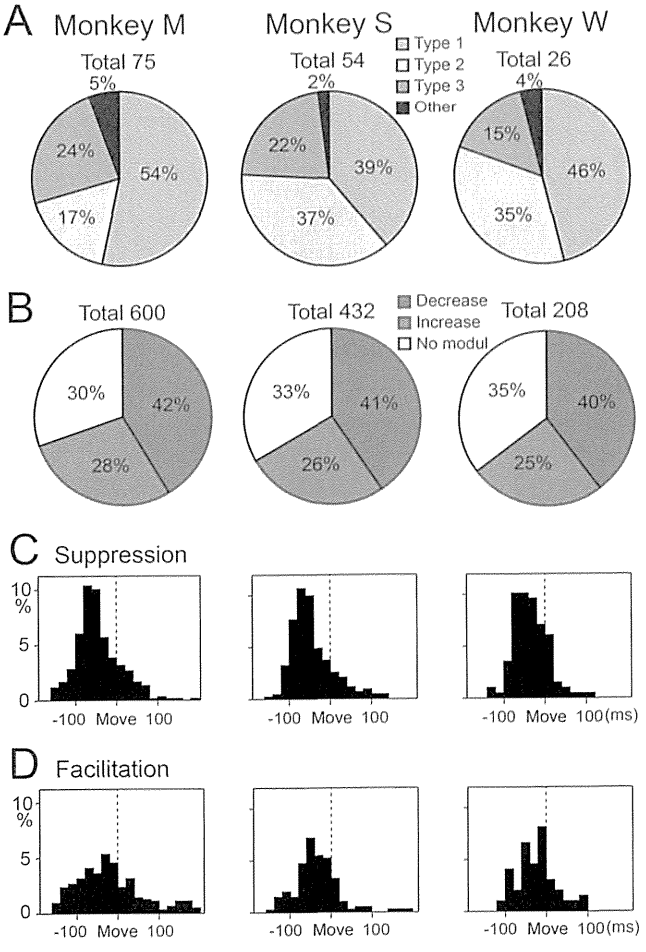


**Figure 6. Percentages of the three types of PCs and distributions of onset latency for all suppressions and facilitations of SS activity.** A: Percentages of the three types of SS activity in the pronated posture in each animal. 'Total' at the top of each pie chart indicates the number of cells. B: Percentages of all facilitations and suppressions among the three types of modulation in the pronated posture in each animal. 'Total' at the top of each pie chart indicates the number of data sets (8 directions × number of cells). C and D: Distribution of onset latencies for all initial suppressions (C) and initial facilitations (D) recorded in the pronated posture for the three animals. Mean onset latencies were significantly earlier for the suppressions (C) than for the facilitations (D) (see Table 2).
doi:10.1371/journal.pone.0108774.g006

normalized the offset level of each histogram to zero by subtracting the average activity during the period of 160 to 220 ms before movement onset. We chose this reference time window because the earliest significant modulations of movement-related activity occurred in the next time bin (i.e., 140 to 160 ms before movement onset) for both PCs and DN cells. We smoothed the histograms with a Savitzky-Golay filter. We defined the onset of modulation as the first bin with an increase or decrease of activity of more than 10 Hz that occurred in three or more successive bins (i.e. ≥60 ms). With this method, the magnitude of the modulation changes exceeded the spontaneous firing rate by at least 2SD during the first three bins in nearly all cases (>95%). The activity in each histogram was digitized into 10 Hz-steps and mapped as a single multi-colored strip for each cell. We placed the strips for cells with initial increases on top and those for cells with initial decreases on bottom. The strips were arranged with the earliest increase at the top and the earliest decrease at the bottom. We made separate pseudo-colored maps for each monkey, movement direction and posture. Then, we converted each map into a graphical display of the numbers of cells with increases or decreases in activity during each time bin.

## Results

### Recording of PC activity

We recorded single unit activity of PCs in the lateral part of lobules V and VI of the right cerebellum (Fig. 1A, B) while monkeys used their right hand to perform wrist movements in eight different directions in two separate forearm postures: pronated and supinated [30,35]. We found 195 PCs (85, 78, 32 in monkeys M, S, W, respectively) that displayed significant changes ($p<0.01$, Student's t-test) in SS activity during the execution period (from Go cue to movement termination) of the task. We also recorded CSs in these PCs.

Among these task-related PCs, 188 cells (80, 76, 32 in monkeys M, S, W, respectively) had somatosensory receptive fields (RFs) on the ipsilateral forearm and/or hand and fingers. These PCs, termed wrist-movement-related, are the focus of the present report. We recorded these PCs both on the surface and in the depth of the folium over a relatively wide area (6–12 mm medio-laterally, 5–6 mm rostro-caudally) (Fig. 1D). In 106/188 PCs, we collected data sets in both postures, whereas in 82/188 PCs, we collected a data set in only one posture. In total, we recorded 294 data sets from 188 PCs. The wrist-movement-related PCs demonstrated relatively high spontaneous SS activity (mean ± SD = 46.5±16.5, 40.2±18.5, 38.0±19.5 Hz in monkey M, S, W, respectively) before the instruction signal, as reported in previous studies [26,27,36]. The average spontaneous SS activities showed no statistical differences among the three animals for the two postures. The remaining task-related PCs in the sample (7/195) had RFs in the upper arm, shoulder, trunk, face/mouth or leg, and were excluded from further analysis.

We also recorded a number of highly task-related MFs in the region containing wrist-movement-related PCs (Fig. 3). These MFs showed directional tuning, posture dependence and peripheral RFs that were similar to the characteristics of task-related cells in our previous recordings from M1 and the ventral premotor (PMv) area [30,32,35]. Therefore, it is likely that the wrist-movement-related PCs are located in the cerebrocerebellar region that receives inputs from the cortical motor areas [37,38,39].

### Classification of SS activity of wrist-movement-related PCs

The wrist-movement-related PCs demonstrated a phasic modulation of their SS activity around movement onset in one or more movement directions. The high spontaneous SS activity of PCs allowed them to have bidirectional modulations, i.e., increases and/or decreases. We classified the wrist-movement-related PCs into three types based on the pre-movement modulation. Type 1 PCs showed a steep pre-movement decrease in SS activity that lasted for ~40–200 ms in one or more directions. The representative type 1 PC (Fig. 4A) showed decreases in SS activity in all eight directions, yet the activity demonstrated directional tuning (Fig. 5A). Modulation onset and depth of suppression varied in different directions. In contrast, type 3 PCs demonstrated an increase in SS activity in one or more directions (Fig. 4C). Type 3 PCs also showed directional tuning of the onset time and amplitude of the increase (Fig. 5C). Type 2 PCs demonstrated an initial decrease in some directions and an increase in other

**Table 1.** Modulation onset of SS activity of PCs for the three animals: Earliest onset of individual PCs.

| Monkey | Cell group | Mean | SD | *n* | Range |
|---|---|---|---|---|---|
| M | PC all | −97.7 | 41.4 | 71 | −150 to −10 |
| | PC inc | −101.0 | 51.7 | 24 | −150 to −10 |
| | PC dec | −95.7 | 33.9 | 47 | −150 to −10 |
| S | PC all | −89.2 | 31.4 | 53 | −150 to −10 |
| | PC inc | −88.2 | 30.1 | 22 | −150 to −30 |
| | PC dec | −90.0 | 33.8 | 31 | −150 to −10 |
| W | PC all | −74.8 | 30.2 | 25 | −130 to −10 |
| | PC inc | −78.9 | 24.7 | 9 | −110 to −50 |
| | PC dec | −72.5 | 33.4 | 16 | −130 to −10 |

Means, SDs and Ranges are in milliseconds. PC all: all PCs. PC inc: PCs showing increased SS activity as the earliest modulation regardless of movement direction. PC dec: PCs showing decreased SS activity as the earliest modulation. *n*: numbers of PCs in individual categories. Note: sum of PC inc and PC dec equals PC all. There was no significant difference between PC inc and PC dec in all three animals ($p>0.21$, 0.80, 0.60 in monkey M, S, W, Mann-Whitney U-test).
doi:10.1371/journal.pone.0108774.t001

directions (Fig. 4B and 5B). Notably, decreases were always more frequent than increases, as in this example.

Because parallel fibers (PFs) make direct, excitatory connections with PCs, we were surprised to find that type 3 PCs (15–24%) made up the smallest proportion of our population. The type 1 PCs (39–54%) were the most common, and the type 2 PCs (17–37%) were intermediate (Fig. 6A). In the pronated posture, decreases (40–42%) in SS activity outnumbered increases (25–28%) in all three monkeys (Fig. 6B). Twenty-five PCs altered their discharge pattern between postures (from type 2 to either type 1 or 3). In general, the three types of PCs were intermingled over a wide area in the presumed cerebrocerebellum (not shown).

We examined the onset timing of the earliest movement-related modulation (i.e. facilitation or suppression) of SS activity for all PCs in each monkey, using the pronated posture (Table 1). We found that onset timing did not differ among the three types, regardless of animal ($p>0.30$, $p>0.26$, $p>0.35$ for monkeys M, S, W respectively, Mann-Whitney U test).

Next, we compared the onset timing of all initial suppressions and all initial facilitations for the population of wrist-movement-related PCs in the pronated posture in the three animals (Fig. 6C, D; Table 2). The onset of suppressions occurred significantly earlier than that of facilitations for the two animals with the largest population of PCs ($p<0.0003$ and $p<0.002$ for monkeys M and S, respectively, Mann-Whitney U test) (Fig. 6C, D; Table 2). Even in the third monkey, suppressions occurred earlier than facilitations, although the difference did not reach significance due to the small number of recorded PCs ($p<0.13$, Monkey W, Mann-Whitney U test) (Table 2). We obtained comparable results for the supinated posture.

## CS activity in wrist-movement-related PCs

Mean firing rate of CSs between −500 and 500 ms relative to movement onset was about 0.6 Hz, and there was no significant difference among movement directions and postures. We calculated the probability of CS firing in 50 ms bins per trial in each movement direction in each PC by dividing the number of CSs in a bin by the number of trials (Fig. 7A). The highest probability occurred around movement onset (from −50 to 50 ms), as described in previous studies (e.g. [36]). In the example of monkey M, the probability of a CS in the time window ranged from 0 to 0.65 (mean ± SD = 0.06±0.09). In other words, the occurrence of CSs was infrequent and inconsistent, even in the PC with the highest probability of CS. The low probability of CSs suggests that CSs did not make a reliable contribution to the activity of DN cells in our well-trained animals.

**Table 2.** Modulation onset of SS activity of PCs for the three animals: Onset of all modulations of all PCs.

| Monkey | Cell group | Mean | SD | *n* | Range |
|---|---|---|---|---|---|
| M | Mod all | −32.9 | 67.8 | 560 | −150 to 190 |
| | Mod inc | −19.3 | 79.3 | 252 | −150 to 190 |
| | Mod dec | −44.0 | 54.3 | 308 | −150 to 190 |
| S | Mod all | −40.9 | 48.3 | 349 | −150 to 190 |
| | Mod inc | −35.5 | 39.0 | 137 | −150 to 130 |
| | Mod dec | −44.3 | 51.4 | 212 | −150 to 190 |
| W | Mod all | −29.9 | 44.8 | 172 | −130 to 110 |
| | Mod inc | −23.3 | 48.0 | 69 | −110 to 90 |
| | Mod dec | −34.3 | 42.3 | 103 | −130 to 110 |

Most PCs showed modulation for two to eight movement directions. Mod all: all modulations. Mod inc: increases in modulation. Mod dec: decreases in modulation. *n*: numbers of modulations in individual categories. See also Fig. 6C and D. There was significant difference between Mod inc and Mod dec in monkey M and S ($p<0.0003$ and 0.002, respectively, Mann-Whitney U-test), but not in monkey W ($p<0.13$, Mann-Whitney U-test).
doi:10.1371/journal.pone.0108774.t002

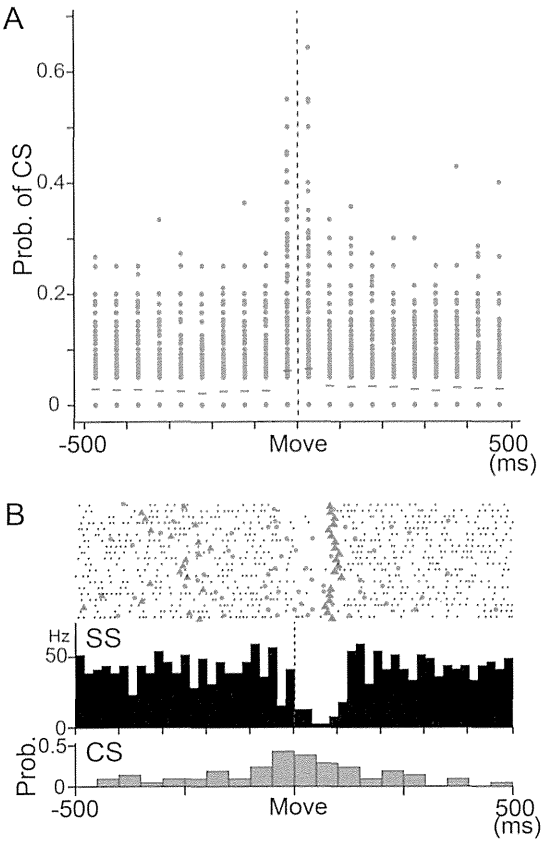


**Figure 7. Movement-related CS activity in PCs.** A: Probability of complex spike firing in 50 ms bins from −500 to 500 ms relative to movement onset in monkey M. Data from all movement directions in all PCs recorded in the pronated posture were plotted (n = 600, 8 directons ×75 PCs) in each bin. A probability of 1 means that a CS was observed in every trial in that time bin for a direction of movement in a PC. Note that the probability was 0 in more than half of PCs in each time bin, except for the bins right before and after movement onset. B: Raster plots and histograms of SS and CS simultaneously recorded in a PC. SS and CS showed a tendency of reciprocal activity around movement onset. Black dots: SS, red dots: CS, gray triangles: Go cue, blue triangles: timing of maximum velocity. Upper histogram: SS activity, 1 bin = 20 ms. Vertical dashed line indicates movement onset. Lower histogram: CS activity, 1 bin = 50 ms. Prob.: probability of occurrence of CS.

doi:10.1371/journal.pone.0108774.g007

## Population activity of the wrist-movement-related SS activity in PCs

To evaluate the entire time course of wrist-movement-related output from PCs to DN cells, we analyzed the modulations of SS activity for the population of wrist-movement-related PCs in each movement direction, posture and animal (8 directions ×2 forearm postures ×3 animals = 48 data sets). We focused on movement-related modulations during the time window from −220 to +300 relative to movement onset. Figure 8A summarizes the modulations of SS activity for 75 PCs recorded from monkey M in four representative directions (UL, UR, DL, DR) in the pronated posture. Movement-related modulations are displayed relative to the averaged activity of each PC during a reference period, 160–220 ms before movement onset (Fig. 8A, *thick black bars above abscissa*). Light/dark blue tiles represent decreases in SS activity, while yellow/red tiles represent increases in SS activity, respectively.

In general, PCs with increases in SS activity and those with decreases began to show significant changes in their firing rate about 160 ms before movement onset (Fig. 9A, blue and red lines). However, shortly thereafter (about 140 ms before movement onset), the graphs show a striking divergence between the numbers of PCs with decreases and those with increases. Before movement onset (from −100 to 0 ms), PCs with decreases in SS activity outnumbered those with increases for all four directions (Fig. 8A, *decreases*: *increases*, UL 28:19; UR 29:22; DL 34:22; DR 31:27). Indeed, the majority of datasets showed a dominance of PCs with decreases in SS activity in this early time period, regardless of animal (Fig. 9A) (20/24 datasets: 7/8 directions in monkey M, 7/8 in monkey S, 6/8 in money W). In contrast, 140–240 ms after movement onset, PCs with increases in SS activity outnumbered those with decreases for all four directions (Fig. 8A, *decreases: increases*, UL 20:29; UR 18:33; DL 17:23; DR 20:27) and for all animals (Fig. 9A). Overall, the PCs with movement-related decreases in SS activity dominated before and for a short period after movement onset, whereas the PCs with increases in SS activity began to dominate ~100 ms after movement onset (Fig. 9A). We obtained comparable results for the supinated posture. Considering the brief velocity pulse and short movement duration of the wrist movements (Fig. 2B and C), we suggest that PC activity before and just after movement onset is associated with execution of the movement, whereas later activity is associated with stopping the movement in the target and maintaining the wrist position at the end of movement.

The difference in the temporal patterns of suppression and facilitation of PCs suggests that the outputs of the PCs to individual DN cells may not cancel each other, even if they converged onto a common DN cell. Because PCs exert a strong inhibition on DN cells, the initial dominance of PCs that show decreased activity may provide excitatory drive to their target DN cells before and just after movement onset. The subsequent dominance of PCs with increased activity may modulate or suppress the preceding activation of DN cells.

## Wrist-movement-related activity of DN cells

In order to examine the proposed mechanisms for cerebellar outputs, we recorded the activity of DCN cells from monkeys M and S during the step-tracking task. We found 192 DCN cells (142 in monkey M, 50 in monkey S) that showed significant task-related modulations. We estimated that these DCN cells were recorded mostly from DN. This estimate is based on their location lateral to the axon bundle in the hilum of DN (Fig. 1B, *h*), along with the chamber maps of the recorded DCN cells (Fig. 1E) and the MRI images for both monkeys (see Materials and Methods). We first excluded fifty-nine DN cells that had RFs in the upper arm, shoulder, face, or leg or were unresponsive to somatosensory stimuli. The remaining 133 task-related DN cells responded strongly to both passive and self-initiated movement of the wrist. Eighty-four of these 133 DN cells showed significant movement-related activity starting before movement onset. Below, we focus on the activity of these 84 "wrist-movement-related" DN cells (65 in monkey M and 19 in monkey S). These wrist-movement-related DN cells demonstrated spontaneous discharges (mean ± SD = 32.4±12.1 Hz, range 8–61 Hz, n = 84), as seen in the examples in Figure 10. The largest modulation of their activity around movement onset (−200 to +200 ms) was comparable with previous studies in DN and IP (mean ± SD = 66.1±25.9 Hz, range 14–147 Hz) [1,2,3,4,5,6,7].

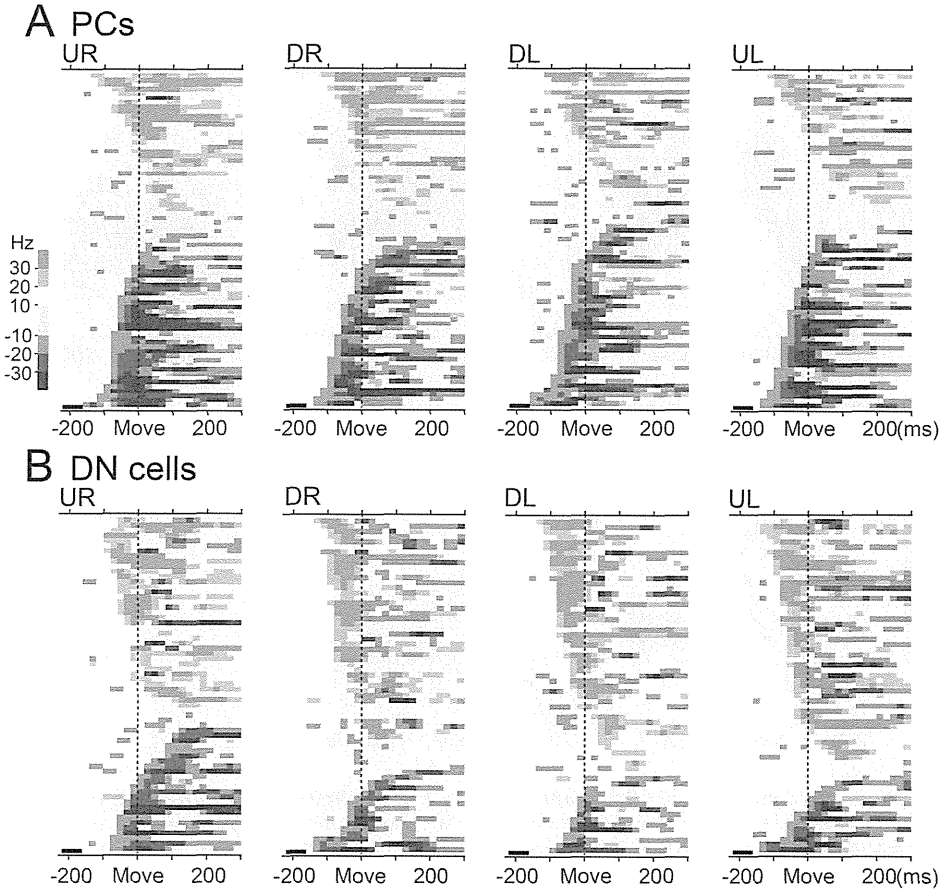


**Figure 8. Modulation of population activity of PCs (A) and DN cells (B) in different movement directions.** Pseudo-color coded summaries of modulation of SS activity of all PCs (A) and activity of all DN cells (B) for four representative targets (UR: upper right, DR: down right, DL: down left, UL: upper left) in the pronated posture in monkey M (see Materials and Methods). Each colored rectangle represents the change in SS activity or DN cell activity relative to a reference period (220 to 160 ms before movement onset, indicated by thick black bar above the abscissa of each diagram). Light/dark blue tiles represent decreases in activity, while yellow/red tiles represent increases in activity. The PCs and DN cells were arranged from top to bottom based on direction of modulation (increase or decrease) and onset time of initial modulation.
doi:10.1371/journal.pone.0108774.g008

## Classification of activity of wrist-movement-related DN cells

We classified the wrist-movement-related DN cells into three types using the same categorization as for the SS activity of PCs. Type 1 DN cells showed a steep decrease in activity that lasted for ~60–200 ms in one or more directions (Fig. 10A). In contrast, type 3 DN cells demonstrated a phasic increase in activity in one or more directions (Fig. 10C). The type 1 and 3 DN cells demonstrated directional tuning of onset time and modulation amplitude (Fig. 11), as we observed in PCs (Fig. 5). Type 2 DN cells demonstrated an increase in some directions and a decrease in other directions (Fig. 11B). Notably, increases were always more frequent than decreases, as in this example. Significantly, most phasic increases in activity of DN cells occurred without evidence of a prior suppression, even on a single-trial basis (Fig. 10B, C). In addition, most DN cells with a movement-related pause of activity did not show a subsequent rebound excitation (Fig. 10A).

We observed a striking difference in the proportions of the 3 neuron-types for the DN cells (Fig. 12A), compared with the PCs (Fig. 6A). The type 2 DN cells (51, 47%) and type 3 DN cells (43, 42%) were quite common, whereas the type 1 DN cells were infrequently observed (6, 11%) in both monkeys (Fig. 12A). Overall, initial increases (58, 54%) outnumbered initial decreases (18, 20%) in the pronated posture for both monkeys (Fig. 12B). In general, the three types of DN cells were intermingled over a wide area (not shown). We analyzed onset timing of the earliest modulations and all initial suppressions and initial facilitations in the two animals, as summarized in Fig. 12C, D and Tables 3 and 4. In striking contrast to the corresponding results for PCs (Fig. 6C, D), we found that the facilitations occurred earlier than the suppressions in DN cells ($p<5.34\times10^{-20}$ and $p<0.09$ for monkeys M and S, respectively, Mann-Whitney U test, Fig. 12C, D). We obtained comparable results for the supinated posture. The finding that facilitations are more numerous and show earlier recruitment than suppressions in DN cells strongly suggests that the primary and major wrist-movement-related output from DN is facilitation.

## Population activity of the wrist-movement-related DN cells

To assess the time course of modulation of activity in the wrist-movement related DN cells, we performed the same analysis as that used for the SS activity of PCs (Fig. 8B). Using the time window of −220 to +300 ms relative to movement onset, we evaluated the modulations of activity for the population of wrist-movement-related DN cells separately for each movement

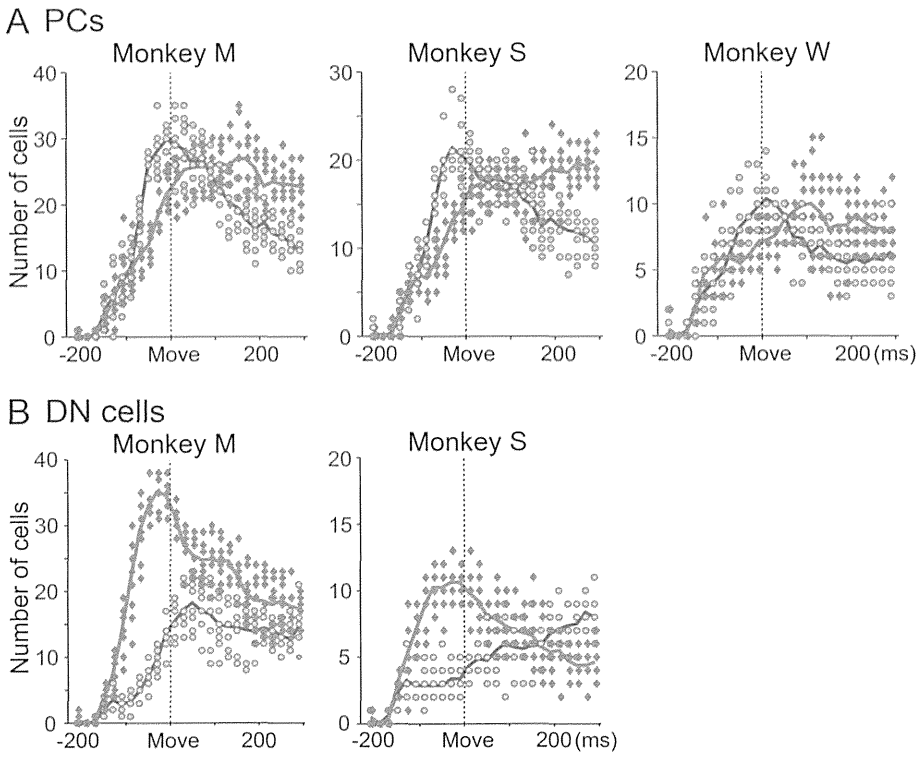


**Figure 9. Temporal patterns of recruitment of all PCs and DN cells with facilitation or suppression of activity for eight different directions.** A: PCs. B: DN cells. In each time bin (20 ms), blue dots represent the number of PCs or DN cells with decreased activity, and red diamonds represent the number of PCs or DN cells with increased activity for eight different directions of movement in the pronated posture in each animal. Blue and red lines indicate mean numbers of blue dots and red diamonds in individual bins, respectively.
doi:10.1371/journal.pone.0108774.g009

direction, posture and animal (8 directions ×2 forearm postures ×2 animals = 32 data sets). Figure 8B summarizes the modulations of activity for 65 DN cells recorded in monkey M in four representative directions (UL, UR, DL, DR) in the pronated posture. The graphs in Fig. 9B show the numbers of DN cells with decreases in activity (blue lines)(Fig. 8B, light/dark blue tiles) and the numbers of DN cells with increases in activity (red lines)(Fig. 8B, yellow/red tiles) separately in each 20 ms time bin. In general, DN cells with increases in activity and those with decreases in activity began to show significant changes in firing rate about 160 ms before movement onset. Significantly, DN cells with increases in activity strongly outnumbered those with decreases in activity throughout the entire movement-related period (Fig. 9B). The dominance of DN cells with increases in activity was greatest before and just after movement onset, and decreased ~100 ms after movement onset (Fig. 9B).

## Relative timing of modulation of the wrist-movement-related PCs and DN cells

We compared the *earliest* modulation for individual PCs and DN cells in monkeys M and S (Tables 1 and 3). We found that the timing of the earliest change in activity for PCs and DN cells did *not* differ significantly in either monkey ($p>0.85$ in monkey M and $p>0.67$ in monkey S, Mann-Whitney U test). We also specifically compared the onset times for the earliest suppressions of PCs and the earliest facilitations of DN cells. The time of onset for the earliest suppressions of PCs and the earliest facilitations of DN cells did not differ significantly in either monkey ($p>0.43$ in monkey M, $p>0.56$ in monkey S, Mann-Whitney U test) (Tables 1 and 3). We obtained comparable results for the supinated posture. Thach [36] also demonstrated that there was no significant difference between onset of PCs and DN cells during arm movements.

## Correspondence between the cerebellar cortex and DN

The PCs and DN cells reported in this study demonstrated significant wrist-movement-related activity and clear somatosensory RFs in the ipsilateral forearm and/or hand and fingers. The PCs were distributed as a large cluster over lobules V and VI (Fig. 1D). The DN cells also were distributed as a large cluster (Fig. 1E). We found PCs and DN cells with RFs in the leg rostral to wrist-movement-related cells and those with RFs in the orofacial region caudal to wrist-movement-related cells (Fig. 1D, E). Thus, both PCs and DN cells displayed a rostro-caudal arrangement of leg, forelimb and orofacial regions, as described in physiological studies [40,41] and an anatomical study [39]. Furthermore, task-related MFs recorded adjacent to the PCs showed pre-movement modulations of activity that were similar to those of task-related cells in M1 and PMv [30,32,35]. The pre-movement modulations of MFs support our view that we recorded PCs mainly from the cerebrocerebellum rather than from the spinocerebellum, where PCs project to IP. Overall, we found a strong functional and morphologic correspondence between the regions in the cerebellar cortex and DN where we recorded wrist-movement-related cell activities.

# Discussion

How do DN cells become active under strong inhibition from PCs? To the best of our knowledge, the present study is the first to address this question by comparing the patterns of activity of PCs

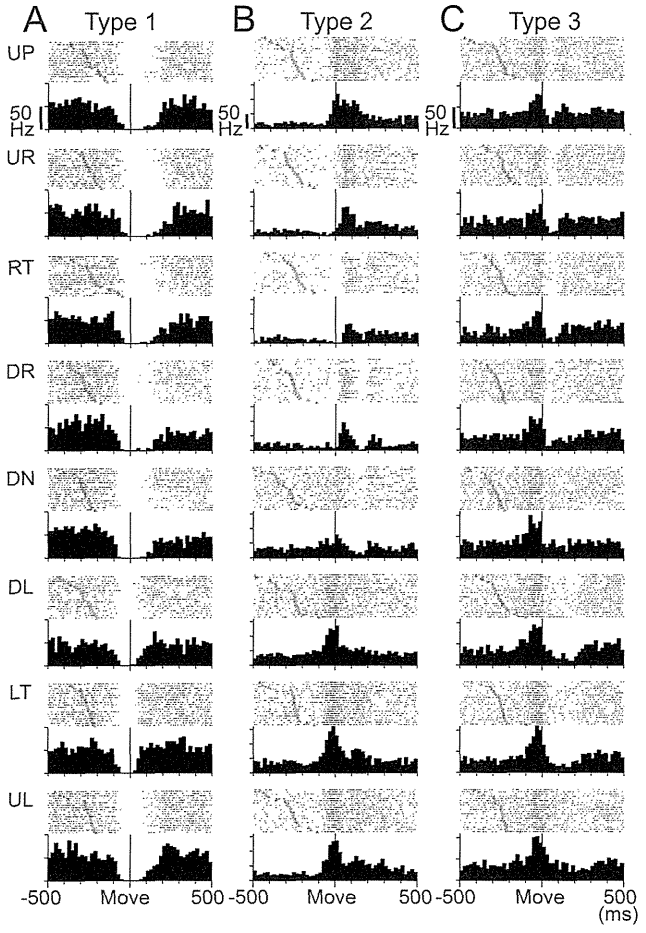


**Figure 10. Three types of activity in wrist-movement-related DN cells.** Raster plots and histograms of typical examples of three types of activity in DN cells with RFs in the distal part of the arm. Neuron activity recorded in the pronated posture is illustrated. DN cells were classified into three types based on movement-related modulations between −200 to +200 ms relative to movement onset. This figure uses the same conventions as Figure 4. A: Activity of type 1 DN cells showed suppression before movement onset. B: Activity of type 2 DN cells showed suppression before movement onset for some directions and facilitation for other directions. C: Activity of type 3 DN cells showed facilitation before movement onset. Note that the scale bars for discharge rate shown in the top row of panels differ for the three cells.

doi:10.1371/journal.pone.0108774.g010

and DN cells in awake animals performing limb movements. We found that the majority of PCs in the cerebrocerebellum were suppressed prior to the onset of rapid wrist movements (Figs. 4A and 6A). At the same time the majority of DN cells were activated without prior suppression (Figs. 10C and 12A). We showed further that the activity of PCs with movement-related suppressions developed earlier than the activity of PCs with movement-related facilitations (Figs. 8A and 9A). Notably, we observed the opposite temporal pattern for the movement-related DN cells, namely, movement-related facilitations became predominant prior to movement-related suppressions (Fig. 8B and 9B). Taken together, our observations suggest that the movement-related activation of DN cells occurs when they are released from tonic inhibition by PCs, i.e. disinhibition. Below we discuss the implications of these results.

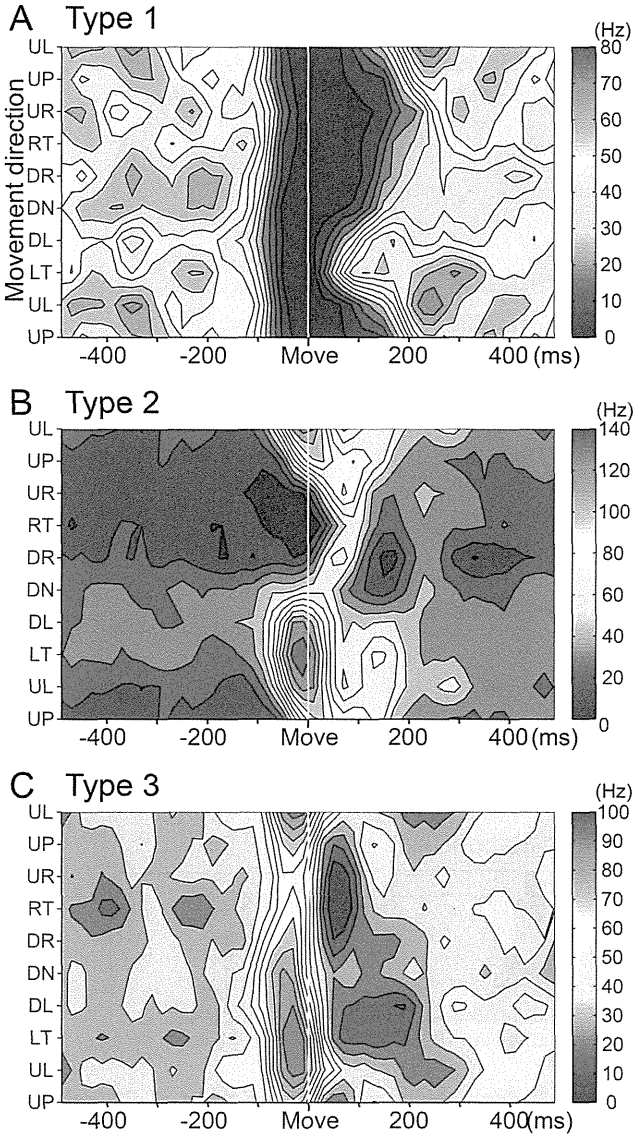


**Figure 11. Contour plots of three types of DN cell activity.** Spatiotemporal maps of neuron activity of type 1 (A), type 2 (B) and type 3 (C) DN cells in relation to 8 movement directions for the same cells illustrated in Figure 10. These plots were generated with MATLAB. Color code was adjusted according to the maximum firing rate in each DN cell.

doi:10.1371/journal.pone.0108774.g011

## Selection of DN

DN is not the only cerebellar nucleus that makes a critical contribution to limb motor control. IP is also important for limb movement [6]. Nevertheless, our selection of DN rather than IP was very critical for this study. IP receives strong MF collateral inputs from various sources such as lateral reticular nucleus [14], external cuneate nucleus [42] or spinal cord [11]. In contrast, DN has long been recognized to have exceptionally weak MF collateral inputs [9,10,11,12,13,14,43]. For instance, less than 10% of MFs from PN send sparse collaterals to DN [13]. Overall, the MF collateral input cannot be the primary determinant of activities of DN cells. Therefore, we focused on the relationship between DN and the corresponding part of the cerebellar cortex.

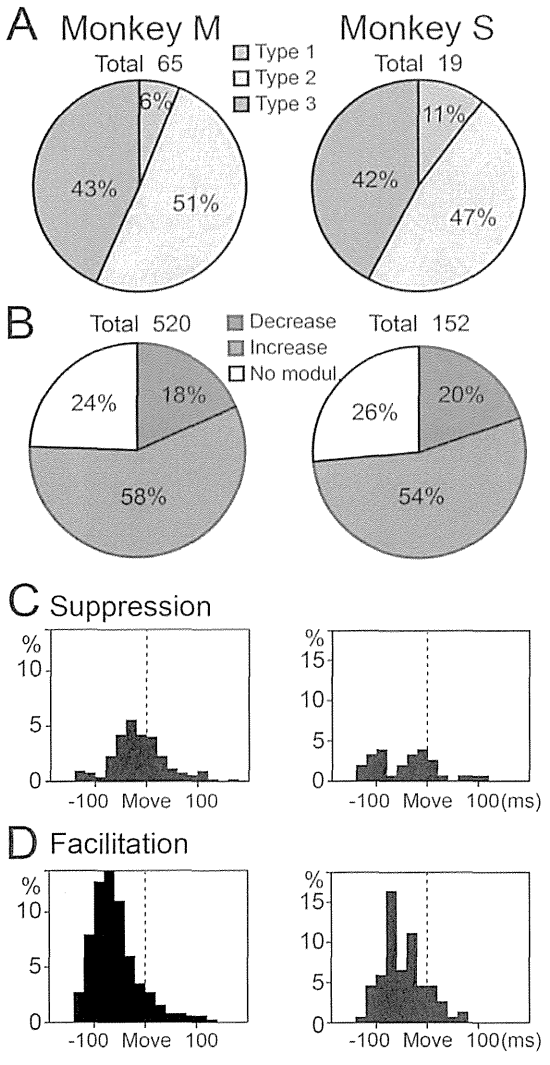


**Figure 12. Percentages of the three types of DN cells and distributions of onset latency for all suppressions and facilitations of DN cell activity.** A: Percentages of the three types of DN cell activity in the pronated posture in monkeys M and S. 'Total' at the top of each pie chart indicates the number of cells. B: Percentages of all facilitations and suppressions among the three types of modulation in the pronated posture in each animal. 'Total' at the top of each pie chart indicates the number of data sets (8 directions × number of cells). C and D: Distribution of onset latencies for all suppressions (C) and facilitations (D) recorded in the pronated posture for the two animals. Mean onset latencies were significantly earlier for the facilitations (D) than for the suppressions (C) (see Table 4).
doi:10.1371/journal.pone.0108774.g012

## Comparing activity of PCs and DN cells during step-tracking movements of the wrist

In a prior study, inactivation of DN made step-tracking arm movements ataxic [8]. Therefore, DN, more generally the cerebrocerebellum, is essential for coordination of the fast and precise movements employed in this study [30,35]. Furthermore, we designed the experiment optimally to compare activities of PCs and DN cells in the same monkey. First, we trained the animals to perform a wide range of wrist movements with stereotyped movement kinematics (Fig. 2), so that we could analyze reproducible neuron activities (e.g., Figs. 4 and 10). Second, we adjusted the location and angle of the recording chamber (see Materials and Methods) to maximize the chance of recording from PCs and DN cells related to movements of the distal forelimb (see Figs. 4 and 8 in Lu et al. [39]). Indeed, in a recent study [32], we reported that a great majority of MFs recorded in the same region of the cerebellar cortex in the same animals (Monkey M and S) showed delay period and/or pre-movement period activities (Fig. 3) that are comparable to those observed in M1 or PMv neurons [30,35]. This result strongly suggests that we recorded PCs in the region of the cerebrocerebellum that is connected to M1 or PMv [38,39]. Overall, the present study is suitable for making precise comparisons of the temporal patterns of movement-related activities in PCs and DN cells.

## Activation of DN cells by disinhibition

Previous authors reported that DN cells become strongly active prior to the onset of limb movements in monkeys [1,2,3,4,5,6,7], as confirmed in this study (Fig. 10). Three mechanisms have been proposed for the excitation of DN cells: 1) collateral inputs from MFs; 2) rebound excitation of DN cells; 3) disinhibition of DN cells. We examined the potential contributions of these mechanisms to DN cell activity by comparing the temporal patterns of movement-related modulations for PCs and DN cells in monkeys performing step-tracking wrist movements.

If activation of DN cells arises mainly from collaterals of the ponto-cerebellar projection, then bursts of activity in DN cells should precede modulation of PCs, as was observed during visually guided saccades in the fastigial oculomotor region and the oculomotor vermis [44]. However, we did not find a significant difference between the earliest modulation of PCs and the earliest modulation of DN cells, as Thach [36] reported previously. In addition, previous morphologic data suggest that the contribution of MF collaterals may be small within DN [13,45,46]. These studies found that DN cells receive a relatively weak projection from a minority of the ponto-cerebellar MFs. Moreover, terminations of the ponto-cerebellar collaterals were located on the distal ends of dendrites of DN cells, which would minimize their synaptic efficacy [47]. Indeed Holdefer et al. (2005) [48] clearly demonstrated that excitatory inputs from MF collaterals were undetectable in DN cells without blocking the strong inhibitory PC input. Therefore, it is unlikely that MF collaterals play a primary role in generating the pre-movement burst of DN cells. Nevertheless, our data may suggest a contribution of collateral input to the pre-movement burst in DN cells. We observed a small dominance of decreases over increases in PCs (Figs. 8A and 9A) and a more marked dominance of increases over decreases in DN cells (Figs. 8B and 9B). This difference is consistent with an additional excitatory input to DN cells that counteracts inhibition by PCs. Therefore, MF collaterals may play an assistive role in activating DN cells, as was demonstrated for IP cells *in vivo* [49].

Second, activation of DN cells may be triggered by a post-inhibitory rebound excitation after a phasic increase of suppression from PCs, as shown *in vitro* [15,16,17] and *in vivo* [16,18,20] experiments with artificial stimuli. However, in the present study performed in behaving monkeys without artificial stimuli, we found that a great majority of PCs exhibited strong suppression of activity before movement onset (Figs. 4A, B and 8A), at the same time that a minority of PCs showed facilitation of activity (Figs. 4C and 8A). Most DN cells showed activation without evidence of prior suppression (Figs. 8B, 10B, C). In addition, most DN cells with a movement-related pause of activity did not show a subsequent rebound excitation (Figs. 8B and 10A). A few DN cells showed a rebound-like activity, but this occurred only *after* movement onset (Fig. 8B). Thus, in behaving monkeys, prior

**Table 3.** Modulation onset of activity of DN cells for the two animals: Earliest onset of individual DN cells.

| Monkey | Cell group | Mean | SD | *n* | Range |
|---|---|---|---|---|---|
| M | DNC all | −93.1 | 29.4 | 65 | −150 to −10 |
| | DNC inc | −95.9 | 26.6 | 51 | −150 to −30 |
| | DNC dec | −82.9 | 37.3 | 14 | −130 to −10 |
| S | DNC all | −92.1 | 38.2 | 19 | −150 to −10 |
| | DNC inc | −85.0 | 37.6 | 16 | −150 to −10 |
| | DNC dec | −130 | — | 3 | −130 |

The same conventions as in Table 1. DNC all: all DN cells. DNC inc: DN cells showing increased activity as the earliest modulation regardless of movement direction. DNC dec: DN cells showing decreased activity as the earliest modulation. There was significant difference between DNC inc and DNC dec in monkey S ($p<0.002$, Mann-Whitney U-test), but not in monkey M ($p<0.27$, Mann-Whitney U-test).
doi:10.1371/journal.pone.0108774.t003

suppression is not required to generate a burst activity in DN cells, and even a complete halt of discharge is not enough to trigger the rebound mechanism of DN cells (Fig. 10A). In agreement with our observations, Alvina et al. [19] demonstrated that rebound firing of DCN cells is not frequently observed even *in vitro*. We note also that rebound firing has been demonstrated in IP, but not in DN where we recorded neurons. Considering the differences in input-output organization of these two nuclei, it is possible that DCN cells in DN and IP differ in their response to inputs from the cerebellar cortex. Overall, we conclude that rebound excitation did not make a major contribution to the generation of the movement-related burst activity of DN cells in our experimental conditions and recording location.

We also evaluated the possibility that synchronized CSs may initiate rebound excitation of DN cells [16,20] through synchronous activation of a population of PCs in our preparation. The firing probability of CSs showed a slight increase in two 50 ms time bins before and after movement onset (Fig. 7A), as was described previously (e.g. [36]). However, a peak firing probability above the chance level (i.e. $p = 0.5$) was extremely rare in either bin, regardless of PC and movement direction. The average firing probability even in these two time windows was only 0.06 and 0.07. Overall, the level of CS activity during our task was far below the synchrony achieved by direct or indirect stimulation of the inferior olive.

Recently, Person and Raman [50,51] demonstrated the possibility of another type of synchronous PC activity to activate DCN cells. This mechanism does not require a preceding increase in activity of individual PCs. Rather, it involves synchronous activity of a number of PCs that project to an individual DN cell. We cannot exclude that this mechanism may contribute to activation of DN cells in awake, behaving animals. However, a great majority of the task-related PCs demonstrated a strong decrease in activity before movement onset (Figs. 4A and 9A), which would minimize the efficacy of synchronous PCs. Overall, synchronous activity of PCs may contribute at best to a fraction of the pre-movement activation of DN cells.

Third, activation of DN cells may be triggered by disinhibition [13,21,25]. Both PCs and DN cells are known to have unusually high spontaneous activities [27]. Indeed, we observed high baseline activity in the PCs (~40 Hz) and DN cells (~30 Hz) recorded in this study. This high activity in PCs would exert a strong tonic suppression of the high intrinsic activity of DN cells. If this is the case, then suppression of PC activity prior to movement onset, as observed in the present and many previous studies [26,29,31,36,52], would disinhibit the target DN cells and release their intrinsic activity. Indeed, DCN cells can be reliably activated by a brief suppression of their inhibitory inputs [53]. Furthermore, transient suppression of PC activity induced prompt activation of DN cells followed by a movement [25]. In this study, a great majority of DN cells generated movement-related bursts of activity without a preceding suppression that is required for rebound excitation. Taken together, our observations suggest that disinhibition plays a primary role in activating DN cells. On the other hand, it should be emphasized that disinhibition and rebound excitation are not mutually exclusive. That is, a *'reduction of inhibition'* triggers excitation of DN cells in either case. As suggested by Bengtsson et al. [20], some ionic mechanisms and conductance machinery underlying rebound excitation could assist in speeding up the response of DCN cells to the fast reduction in SS activity of PCs that we observed. The two mechanisms may be distinguishable by careful examination of the temporal features of

**Table 4.** Modulation onset of activity of DN cells for the two animals: Onset of all modulations of all DN cells.

| Monkey | Cell group | Mean | SD | *n* | Range |
|---|---|---|---|---|---|
| M | Mod all | −44.7 | 53.9 | 484 | −150 to 190 |
| | Mod inc | −58.5 | 47.6 | 335 | −150 to 190 |
| | Mod dec | −13.6 | 54.6 | 149 | −130 to 130 |
| S | Mod all | −56.4 | 35.9 | 128 | −150 to 110 |
| | Mod inc | −62.4 | 35.9 | 90 | −150 to 50 |
| | Mod dec | −42.1 | 35.6 | 38 | −130 to 110 |

Most DN cells showed modulation for two to eight movement directions. Mod all: all modulations. Mod inc: increases in modulation. Mod dec: decreases in modulation. See also Fig. 12C and D. Mod inc occurred earlier than Mod dec in monkey M and S ($p<5.3\times10^{-20}$ and 0.09, respectively, Mann-Whitney U-test).
doi:10.1371/journal.pone.0108774.t004

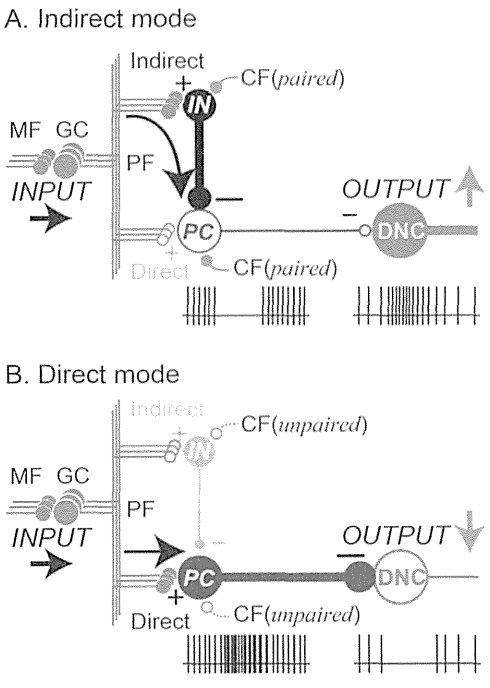


**Figure 13. Parallel pathways in the cerebellar cortex determine two modes of DN cell (DNC) output.** A. Indirect mode. B. Direct mode. This is a summary diagram of the functional organization of the cerebellum supported by this study. In the cerebellar cortex, mossy fiber (MF) inputs (INPUT) are relayed by granule cells (GCs) and are processed differently through two parallel pathways, an indirect pathway (Indirect) and a direct pathway (Direct). In the indirect pathway, parallel fiber (PF) inputs activate interneurons (INs) that suppress PCs. Because PC activity provides a tonic suppression of DNCs, the suppression of PC activity facilitates DNCs through disinhibition (A, OUTPUT ↑). In the direct pathway, PF inputs excite PCs directly. Because PCs are inhibitory, their activation suppresses the DNCs (B, OUTPUT ↓). The balance between the two pathways determines the final output patterns of individual PCs. In this way, inhibitory PCs are able to exert bidirectional effects on DNCs and enable a variety of cerebellar output patterns. CF: climbing fiber. Paired: CF activity paired with PF inputs. Unpaired: CF activity unpaired with PF inputs. Pluses (+) represent excitatory synapses, and minuses (−) represent inhibitory synapses. Note that, in this diagram the PC and the IN share inputs from the same PFs. This is meant to show the basic connectivity of the cerebellar cortex in the simplest form. In reality, a PC and an associated IN may or may not have common PF inputs.
doi:10.1371/journal.pone.0108774.g013

modulation of PCs and DN cells. However, disinhibition might activate DN cells with only a synaptic delay (~1 ms), which would be undetectable in our experimental setup. On the other hand, a rebound response requires a strong inhibition of longer duration (>10 ms, e.g. Hoebeek et al. [16]) before activation of DN cells. Future experiments comparing activities of PCs and DN cells with identified connectivity will be needed to confirm our conclusion that DN cells are most likely activated by disinhibition.

Why has suppression of SS activity attracted relatively little attention so far? For a long time, it was assumed that the *primary* modulation of SS activity was an increase. Previous studies reported increases of SS activity in behaving monkeys for arm movements [26,36,54,55,56] and eye movements [44,57,58]. Nevertheless, all of these studies also noted a considerable or even comparable number of PCs with decreases in SS activity. Harvey et al. [56] and Espinoza and Smith [55] reported that 40% and 44% of the arm-movement-related PCs showed decreases in SS activity, respectively. Similarly, Coltz et al. [54] reported that 41% of PCs showed a decrease in SS activity for increases in arm velocity. In the present study, about 55% of all initial modulations of wrist-movement-related SS activity were suppressions (Fig. 6B) in all three monkeys. Overall, for studies that analyzed arm movements, the emphasis on increases in SS activity may have resulted largely from a historical focus on excitation, rather than on a difference in observations between prior experiments and ours.

The early, strong suppression of SS activity observed in this study is likely to be mediated by molecular layer interneurons (INs), especially basket cells [59]. It is commonly thought that monosynaptic activation of PCs should precede disynaptic inhibition of PCs by a few milliseconds, but our results indicate that the disynaptic pathway may be recruited faster than expected. We suggest that multiple mechanisms may shorten the delay in the disynaptic pathway, as reviewed by Jörntell et al. [59]. First, there is evidence that EPSPs from PFs are large and have a fast rise time in INs, which facilitates a very rapid spike initiation in INs [60,61,62]. Second, axon terminals of INs wrap around somata and initial segments of PCs [63] and provide exceptionally effective inhibition of PCs [64,65]. Taken together, these features suggest that the disynaptic inhibitory pathway is optimally designed to provide fast, strong and precisely timed inhibition of PCs and result in burst activity in DCN cells via disinhibition [25]. Indeed, Ebner and his colleagues clearly demonstrated that stimulation of a PF beam induced disynaptic inhibition of PCs at a *lower* threshold than was needed for direct excitation of PCs (Fig. 7 in Gao et al. [66]). The lower threshold of PC inhibition is consistent with our suggestion that the inhibitory pathway is recruited earlier in behaving monkeys.

## Asymmetric processing through parallel pathways in the cerebellar cortex

MF inputs to the cerebellar cortex are relayed by GCs and then processed in two *parallel pathways* to PCs (Fig. 13) [67]. The *direct pathway* activates PCs directly, while the *indirect pathway* uses inhibitory INs to suppress PCs. Dean et al. [67] proposed that the parallel pathways work in a cooperative way to suppress or facilitate activity of PCs in the cerebellar cortex. Based on our observations, we extend their idea to explain the role of the parallel pathways for generation of cerebellar output from DN. The parallel pathways provide two modes for transforming MF inputs to DCN outputs though PCs (Fig. 13). Because PC outputs are inhibitory, excitation of PCs through the direct pathway suppresses their target DN cells, and suppression of PCs through the indirect pathway facilitates their target DN cells. We found that movement-related suppressions of SS activity dominated before movement onset and movement-related excitations dominated after movement onset in our population of PCs (Figs. 8A and 9A). We propose that the indirect pathway plays the leading role in initiating cerebellar outputs for limb movements.

In this study, we focused on modulation of SS activity of PCs. Nevertheless, we need to discuss CF inputs and relevant synaptic plasticity to understand how the two modes of SS modulation are acquired (Fig. 13). It is generally accepted that CF inputs have reciprocal effects on PF inputs to INs and PCs [61,68,69,70,71]. Stimulation of a PF input *paired* with CF activity induces LTP of PF-IN synapses and LTD of PF-PC synapses. Therefore, it is likely that decreases in SS activity are developed by repetitive *paired* activation of PF and CF inputs. In contrast, stimulation of a PF input *unpaired* with CF activity induces LTD of PF-IN synapses and LTP of PF-PC synapses. Therefore, it is likely that increases in SS activity are developed by repetitive *unpaired* activation of PF and CF inputs. For this reciprocity in development of plasticity to

occur, PCs showing decreases in SS activity and PCs showing increases in SS activity concurrently should be innervated by distinct CFs with a low or even negative correlation.

Several prior studies have provided strong support for the reciprocity between CS activity and SS activity of a PC. For instance, CS activity and SS activity in individual PCs showed reciprocal activities during ocular following [72], smooth pursuit [73] and limb movements [31,36,74] (see also Fig. 7B). Furthermore, during saccadic adaptation, adaptive changes of CS activity and SS activity demonstrated a negative correlation [75].

### Consideration of the operating principle of the cerebrocerebellum

The cerebellum has long been regarded as "neural machinery" designed to process input information in some unique and essential manner [76]. In this regard, it is most important to determine the primary mode of operation of the inhibitory PC in the cerebrocerebellum. The PC determines how movement-related information is represented, processed and output from DCN, thereby defining the functional organization of the cerebrocerebellum. To our knowledge, previous studies gave greater attention to facilitation of the PC as the *primary* modulation and understated suppression of the PC, despite repeated observations of suppression of SS activity in voluntary arm movements [26,29,31,36,52]. The bias toward facilitation of SS activity is understandable because electrical PF stimulation induced an initial excitation and later inhibition of PCs in anesthetized animals [77]. In the present study, we have clearly demonstrated that the primary modulation of the PC in the cerebrocerebellum is suppression of SS activity for execution of wrist movements in behaving monkeys. As a result, we propose that output from the DN is primarily triggered by disinhibition. Our results provide a new perspective on the mechanisms used by PCs to influence limb motor control and on the plastic changes that underlie motor learning in the cerebellum.

## Acknowledgments

We thank Dr. Peter L. Strick for his continuous encouragement during this research and for invaluable advice. We thank Dr. Richard Dum for his insightful comments and advice on each version of the manuscript. We also thank Drs. Masao Ito and Tadashi Yamazaki for their invaluable comments on this manuscript. We thank Drs. Hiroyuki Takuwa and Wataru Matsui for their help in an initial part of the experiment. We thank Dr. Toshio Iijima for his support for an initial part of the experiment.

## Author Contributions

Conceived and designed the experiments: SK. Performed the experiments: TI ST YT JL SK. Analyzed the data: TI ST YT DH SK. Wrote the paper: SK TI DH. Designed the software used in analysis: TI.

## References

1. Chapman CE, Spidalieri G, Lamarre Y (1986) Activity of dentate neurons during arm movements triggered by visual, auditory, and somesthetic stimuli in the monkey. J Neurophysiol 55: 203–226.
2. Fortier PA, Kalaska JF, Smith AM (1989) Cerebellar neuronal activity related to whole-arm reaching movements in the monkey. J Neurophysiol 62: 198–211.
3. Goodkin HP, Thach WT (2003) Cerebellar control of constrained and unconstrained movements. II. EMG and nuclear activity. J Neurophysiol 89: 896–908.
4. Strick PL (1983) The influence of motor preparation on the response of cerebellar neurons to limb displacements. J Neurosci 3: 2007–2020.
5. Thach WT (1970) Discharge of cerebellar neurons related to two maintained postures and two prompt movements. I. Nuclear cell output. J Neurophysiol 33: 527–536.
6. van Kan PL, Houk JC, Gibson AR (1993) Output organization of intermediate cerebellum of the monkey. J Neurophysiol 69: 57–73.
7. Wetts R, Kalaska JF, Smith AM (1985) Cerebellar nuclear cell activity during antagonist cocontraction and reciprocal inhibition of forearm muscles. J Neurophysiol 54: 231–244.
8. Vilis T, Hore J (1977) Effects of changes in mechanical state of limb on cerebellar intention tremor. J Neurophysiol 40: 1214–1224.
9. Dietrichs E, Bjaalie JG, Brodal P (1983) Do pontocerebellar fibers send collaterals to the cerebellar nuclei? Brain Res 259: 127–131.
10. Glickstein M (1997) Mossy-fibre sensory input to the cerebellum. Prog Brain Res 114: 251–259.
11. Matsushita M, Xiong G (2001) Uncrossed and crossed projections from the upper cervical spinal cord to the cerebellar nuclei in the rat, studied by anterograde axonal tracing. J Comp Neurol 432: 101–118.
12. Shinoda Y, Izawa Y, Sugiuchi Y, Futami T (1997) Functional significance of excitatory projections from the precerebellar nuclei to interpositus and dentate nucleus neurons for mediating motor, premotor and parietal cortical inputs. Prog Brain Res 114: 193–207.
13. Shinoda Y, Sugiuchi Y, Futami T, Izawa R (1992) Axon collaterals of mossy fibers from the pontine nucleus in the cerebellar dentate nucleus. J Neurophysiol 67: 547–560.
14. Wu HS, Sugihara I, Shinoda Y (1999) Projection patterns of single mossy fibers originating from the lateral reticular nucleus in the rat cerebellar cortex and nuclei. J Comp Neurol 411: 97–118.
15. Aizenman CD, Linden DJ (1999) Regulation of the rebound depolarization and spontaneous firing patterns of deep nuclear neurons in slices of rat cerebellum. J Neurophysiol 82: 1697–1709.
16. Hoebeek FE, Witter L, Ruigrok TJ, De Zeeuw CI (2010) Differential olivocerebellar cortical control of rebound activity in the cerebellar nuclei. Proc Natl Acad Sci USA 107: 8410–8415.
17. Tadayonnejad R, Anderson D, Molineux ML, Mehaffey WH, Jayasuriya K, et al. (2010) Rebound discharge in deep cerebellar nuclear neurons in vitro. Cerebellum 9: 352–374.
18. Witter L, Canto CB, Hoogland TM, de Gruijl JR, De Zeeuw CI (2013) Strength and timing of motor responses mediated by rebound firing in the cerebellar nuclei after Purkinje cell activation. Front Neural Circuits 7: 133.
19. Alvina K, Walter JT, Kohn A, Ellis-Davies G, Khodakhah K (2008) Questioning the role of rebound firing in the cerebellum. Nat Neurosci 11: 1256–1258.
20. Bengtsson F, Ekerot CF, Jörntell H (2011) In vivo analysis of inhibitory synaptic inputs and rebounds in deep cerebellar nuclear neurons. PLoS One 6: e18822.
21. Albus JS (1971) A Theory of Cerebellar Function. Mathematical Biosciences 10: 25–61.
22. Medina JF, Mauk MD (2000) Computer simulation of cerebellar information processing. Nat Neurosci 3 Suppl: 1205–1211.
23. Miyashita Y, Nagao S (1984) Contribution of cerebellar intracortical inhibition to Purkinje cell response during vestibulo-ocular reflex of alert rabbits. J Physiol 351: 251–262.
24. Nagao S (1992) Different roles of flocculus and ventral paraflocculus for oculomotor control in the primate. Neuroreport 3: 13–16.
25. Heiney SA, Kim J, Augustine GJ, Medina JF (2014) Precise control of movement kinematics by optogenetic inhibition of purkinje cell activity. J Neurosci 34: 2321–2330.
26. Mano N, Yamamoto K (1980) Simple-spike activity of cerebellar Purkinje cells related to visually guided wrist tracking movement in the monkey. J Neurophysiol 43: 713–728.
27. Thach WT (1968) Discharge of Purkinje and cerebellar nuclear neurons during rapidly alternating arm movements in the monkey. J Neurophysiol 31: 785–797.
28. Ojakangas CL, Ebner TJ (1992) Purkinje cell complex and simple spike changes during a voluntary arm movement learning task in the monkey. J Neurophysiol 68: 2222–2236.
29. Yamamoto K, Kawato M, Kotosaka S, Kitazawa S (2007) Encoding of movement dynamics by Purkinje cell simple spike activity during fast arm movements under resistive and assistive force fields. J Neurophysiol 97: 1588–1599.
30. Kakei S, Hoffman DS, Strick PL (1999) Muscle and movement representations in the primary motor cortex. Science 285: 2136–2139.
31. Kitazawa S, Kimura T, Yin PB (1998) Cerebellar complex spikes encode both destinations and errors in arm movements. Nature 392: 494–497.
32. Ishikawa T, Tomatsu S, Tsunoda Y, Hoffman DS, Kakei S (2014) Mossy fibers in the cerebellar hemisphere show delay activity in a delayed response task. Neurosci Res doi: 10.1016/j.neures.2014.07.006
33. Walsh JV, Houk JC, Mugnaini E (1974) Identification of unitary potentials in turtle cerebellum and correlations with structures in granular layer. J Neurophysiol 37: 30–47.
34. Crammond DJ, Kalaska JF (1996) Differential relation of discharge in primary motor cortex and premotor cortex to movements versus actively maintained postures during a reaching task. Exp Brain Res 108: 45–61.
35. Kakei S, Hoffman DS, Strick PL (2001) Direction of action is represented in the ventral premotor cortex. Nat Neurosci 4: 1020–1025.

36. Thach WT (1970) Discharge of cerebellar neurons related to two maintained postures and two prompt movements. II. Purkinje cell output and input. J Neurophysiol 33: 537–547.
37. Hashimoto M, Takahara D, Hirata Y, Inoue K, Miyachi S, et al. (2010) Motor and non-motor projections from the cerebellum to rostrocaudally distinct sectors of the dorsal premotor cortex in macaques. Eur J Neurosci 31: 1402–1413.
38. Kelly RM, Strick PL (2003) Cerebellar loops with motor cortex and prefrontal cortex of a nonhuman primate. J Neurosci 23: 8432–8444.
39. Lu X, Miyachi S, Ito Y, Nambu A, Takada M (2007) Topographic distribution of output neurons in cerebellar nuclei and cortex to somatotopic map of primary motor cortex. Eur J Neurosci 25: 2374–2382.
40. Mano N (1984) The cerebellum and the voluntary movement - The progress in the last decade. Shinkei Kenkyu no Shinpo 28: 87–102.
41. Thach WT, Perry JG, Schieber MH (1982) Cerebellar output: body maps and muscle spindles. In: Palay SL, Chan-Palay V, editors. The Cerebellum: new vistas. New York: Springer-Verlag. pp. 440–454.
42. Casabona A, Valle MS, Bosco G, Perciavalle V (2008) Comparison of neuronal activities of external cuneate nucleus, spinocerebellar cortex and interpositus nucleus during passive movements of the rat's forelimb. Neuroscience 157: 271–279.
43. Allen GI, Tsukahara N (1974) Cerebrocerebellar communication systems. Physiol Rev 54: 957–1006.
44. Ohtsuka K, Noda H (1995) Discharge properties of Purkinje cells in the oculomotor vermis during visually guided saccades in the macaque monkey. J Neurophysiol 74: 1828–1840.
45. Brodal P, Bjaalie JG (1992) Organization of the pontine nuclei. Neurosci Res 13: 83–118.
46. Shinoda Y, Sugihara I (2012) Axonal trajectories of single climbing and mossy fiber neurons in the cerebellar cortex and nucleus. Handbook of the Cerebellum and Cerebellar Disorders: Springer Science+Business Media, LLC.
47. Chan-Palay V (1977) Cerebellar Dentate Neucleus: Organization, Cytology and Transmitters. New York: Springer-Verlag.
48. Holdefer RN, Houk JC, Miller LE (2005) Movement-related discharge in the cerebellar nuclei persists after local injections of GABA(A) antagonists. J Neurophysiol 93: 35–43.
49. Bengtsson F, Jorntell H (2014) Specific relationship between excitatory inputs and climbing fiber receptive fields in deep cerebellar nuclear neurons. PLoS One 9: e84616.
50. Person AL, Raman IM (2012) Synchrony and neural coding in cerebellar circuits. Front Neural Circuits 6: 97.
51. Person AL, Raman IM (2012) Purkinje neuron synchrony elicits time-locked spiking in the cerebellar nuclei. Nature 481: 502–505.
52. Roitman AV, Pasalar S, Johnson MT, Ebner TJ (2005) Position, direction of movement, and speed tuning of cerebellar Purkinje cells during circular manual tracking in monkey. J Neurosci 25: 9244–9257.
53. Gauck V, Jaeger D (2000) The control of rate and timing of spikes in the deep cerebellar nuclei by inhibition. J Neurosci 20: 3006–3016.
54. Coltz JD, Johnson MT, Ebner TJ (1999) Cerebellar Purkinje cell simple spike discharge encodes movement velocity in primates during visuomotor arm tracking. J Neurosci 19: 1782–1803.
55. Espinoza E, Smith AM (1990) Purkinje cell simple spike activity during grasping and lifting objects of different textures and weights. J Neurophysiol 64: 698–714.
56. Harvey RJ, Porter R, Rawson JA (1977) The natural discharges of Purkinje cells in paravermal regions of lobules V and VI of the monkey's cerebellum. J Physiol 271: 515–536.
57. Stone LS, Lisberger SG (1990) Visual responses of Purkinje cells in the cerebellar flocculus during smooth-pursuit eye movements in monkeys. I. Simple spikes. J Neurophysiol 63: 1241–1261.
58. Soetedjo R, Fuchs AF (2006) Complex spike activity of purkinje cells in the oculomotor vermis during behavioral adaptation of monkey saccades. J Neurosci 26: 7741–7755.
59. Jörntell H, Bengtsson F, Schonewille M, De Zeeuw CI (2010) Cerebellar molecular layer interneurons - computational properties and roles in learning. Trends Neurosci 33: 524–532.
60. Carter AG, Regehr WG (2002) Quantal events shape cerebellar interneuron firing. Nat Neurosci 5: 1309–1318.
61. Jörntell H, Ekerot CF (2003) Receptive field plasticity profoundly alters the cutaneous parallel fiber synaptic input to cerebellar interneurons in vivo. J Neurosci 23: 9620–9631.
62. Llano I, Gerschenfeld HM (1993) Inhibitory synaptic currents in stellate cells of rat cerebellar slices. J Physiol 468: 177–200.
63. Ramón y Cajal S (1911) Histologie du Système Nerveux de l'homme et des Vertébrés. Vol. II. Paris: Maloine.
64. Korn H, Axelrad H (1980) Electrical inhibition of Purkinje cells in the cerebellum of the rat. Proc Natl Acad Sci USA 77: 6244–6247.
65. Blot A, Barbour B (2014) Ultra-rapid axon-axon ephaptic inhibition of cerebellar Purkinje cells by the pinceau. Nat Neurosci 17: 289–295.
66. Gao W, Chen G, Reinert KC, Ebner TJ (2006) Cerebellar cortical molecular layer inhibition is organized in parasagittal zones. J Neurosci 26: 8377–8387.
67. Dean P, Porrill J, Ekerot CF, Jörntell H (2010) The cerebellar microcircuit as an adaptive filter: experimental and computational evidence. Nat Rev Neurosci 11: 30–43.
68. Jörntell H, Ekerot CF (2002) Reciprocal bidirectional plasticity of parallel fiber receptive fields in cerebellar Purkinje cells and their afferent interneurons. Neuron 34: 797–806.
69. Smith SL, Otis TS (2005) Pattern-dependent, simultaneous plasticity differentially transforms the input-output relationship of a feedforward circuit. Proc Natl Acad Sci USA 102: 14901–14906.
70. Szapiro G, Barbour B (2007) Multiple climbing fibers signal to molecular layer interneurons exclusively via glutamate spillover. Nat Neurosci 10: 735–742.
71. Rancillac A, Crepel F (2004) Synapses between parallel fibres and stellate cells express long-term changes in synaptic efficacy in rat cerebellum. J Physiol 554: 707–720.
72. Kobayashi Y, Kawano K, Takemura A, Inoue Y, Kitama T, et al. (1998) Temporal firing patterns of Purkinje cells in the cerebellar ventral paraflocculus during ocular following responses in monkeys II. Complex spikes. J Neurophysiol 80: 832–848.
73. Yang Y, Lisberger SG (2013) Interaction of plasticity and circuit organization during the acquisition of cerebellum-dependent motor learning. Elife 2: e01574.
74. Mano N, Kanazawa I, Yamamoto K (1986) Complex-spike activity of cerebellar Purkinje cells related to wrist tracking movement in monkey. J Neurophysiol 56: 137–158.
75. Catz N, Dicke PW, Thier P (2008) Cerebellar-dependent motor learning is based on pruning a Purkinje cell population response. Proc Natl Acad Sci USA 105: 7309–7314.
76. Eccles J, Ito M, Szentagothai J (1967) The cerebellum as a neuronal machine. New York: Springer-Verlag.
77. Eccles JC, Llinas R, Sasaki K (1966) Intracellularly recorded responses of the cerebellar Purkinje cells. Exp Brain Res 1: 161–183.

Neuroscience Research 87 (2014) 84–89

Contents lists available at ScienceDirect

Neuroscience Research

journal homepage: www.elsevier.com/locate/neures

Rapid Communication

# Mossy fibers in the cerebellar hemisphere show delay activity in a delayed response task

Takahiro Ishikawa[a,*], Saeka Tomatsu[b], Yoshiaki Tsunoda[c], Donna S. Hoffman[d,e], Shinji Kakei[a]

[a] Motor Disorders Project, Tokyo Metropolitan Institute of Medical Science, Tokyo 156-8506, Japan
[b] Department of Neurophysiology, National Institute of Neuroscience, National Center of Neurology and Psychiatry, Tokyo 187-8502, Japan
[c] Frontal Lobe Function Project, Tokyo Metropolitan Institute of Medical Science, Tokyo 156-8506, Japan
[d] Department of Neurobiology, University of Pittsburgh School of Medicine, Pittsburgh, PA 15261, USA
[e] Center for the Neural Basis of Cognition, University of Pittsburgh School of Medicine, Pittsburgh, PA 15261, USA

ARTICLE INFO

*Article history:*
Received 15 May 2014
Received in revised form 20 June 2014
Accepted 17 July 2014
Available online 1 August 2014

*Keywords:*
Cerebellar hemisphere
Mossy fiber
Motor control
Delay period

ABSTRACT

To examine whether mossy fibers (MFs) in the cerebellar hemisphere show delay activity, we recorded MF activity during a wrist movement task with a random instructed delay period in two monkeys. Among 155 task-related MFs, 70 MFs (45%) demonstrated significant delay activity. Those MFs were widely distributed in the cerebellar hemisphere. Some of the activities were evoked by instruction cue presentation, whereas other activity started in anticipation of the upcoming go signal. For most MFs, the delay activities showed directional tuning. These patterns of the activity were in common with those of neurons in the cerebral motor cortices.



Some neurons in the primary motor cortex (M1) and premotor cortex (PM) show prolonged activity between instruction cue presentation and go signal, i.e. delay period activity (Tanji and Evarts, 1976; Weinrich and Wise, 1982; Kurata and Wise, 1988; Crammond and Kalaska, 1994; Kakei et al., 1999, 2001; Nakayama et al., 2008; Kurata, 2010). This activity is thought to be involved in motor planning and/or preparation for upcoming movement (Hoshi and Tanji, 2002). Considering that the cerebral motor cortices send projections to many brain regions, the delay activity may be conveyed to those regions. The hemispheric portions of the cerebellum are a major target of projections from the motor cortices (Kelly and Strick, 2003). This part of the cerebellum receives primary inputs from motor cortices via pontine nuclei (PN), and the ponto-cerebellar tract terminates as mossy fibers (MFs) in the granular layer in the cerebellar cortex. Therefore, MF activity is thought to be modulated by inputs from motor cortices. To examine whether the delay activity is maintained in inputs from motor cortices to the cerebellum, we investigated MF activity during the delay period of a motor task.

We trained two monkeys to perform step-tracking movements of the wrist with a random instructed delay period. Detailed experimental procedures were described in a previous paper (Kakei et al., 1999). Briefly, monkeys sat in a primate chair and faced a monitor that displayed a cursor and a target. Their right forearm was fixed in the pronated posture, and they grasped a manipulandum which interfaced wrist angle and position of the cursor. The monkeys began the task by placing the cursor in the center target. After a variable hold period (800–1200 ms), a peripheral target appeared (instruction cue). The peripheral target was randomly selected from eight possible locations spaced at 45° intervals. Following a variable delay period (1000–2000 ms), the center target disappeared (go signal). Duration of the delay period was adjusted to be distributed within the range so that mean duration of the late delay period should be ~500 ms (see Fig. 2A). Monkeys were allowed 500 ms to initiate a movement and another 500 ms to complete the movement from the center to peripheral target. Each successful movement was rewarded with a drop of juice. We recorded MF activity from the ipsilateral cerebellar hemisphere with glass-coated Elgiloy electrodes (0.8–1.8 MΩ). MF activity was identified based on their characteristic spike waveform (see Fig. 1D in van Kan et al., 1993). MF activities exhibited a short positive-negative potential followed by a longer negative afterwave as shown in previous studies (Walsh et al., 1974; Bourbonnais et al., 1986; Taylor et al., 1987). Because the negative afterwave is considered

* Corresponding author at: Motor Disorders Project, Tokyo Metropolitan Institute of Medical Science, 2-1-6 Kamikitazawa, Setagaya-ku, Tokyo 156-8506, Japan.
Tel.: +81 368342343; fax: +81 353163150.
*E-mail address:* ishikawa-tk@igakuken.or.jp (T. Ishikawa).

http://dx.doi.org/10.1016/j.neures.2014.07.006

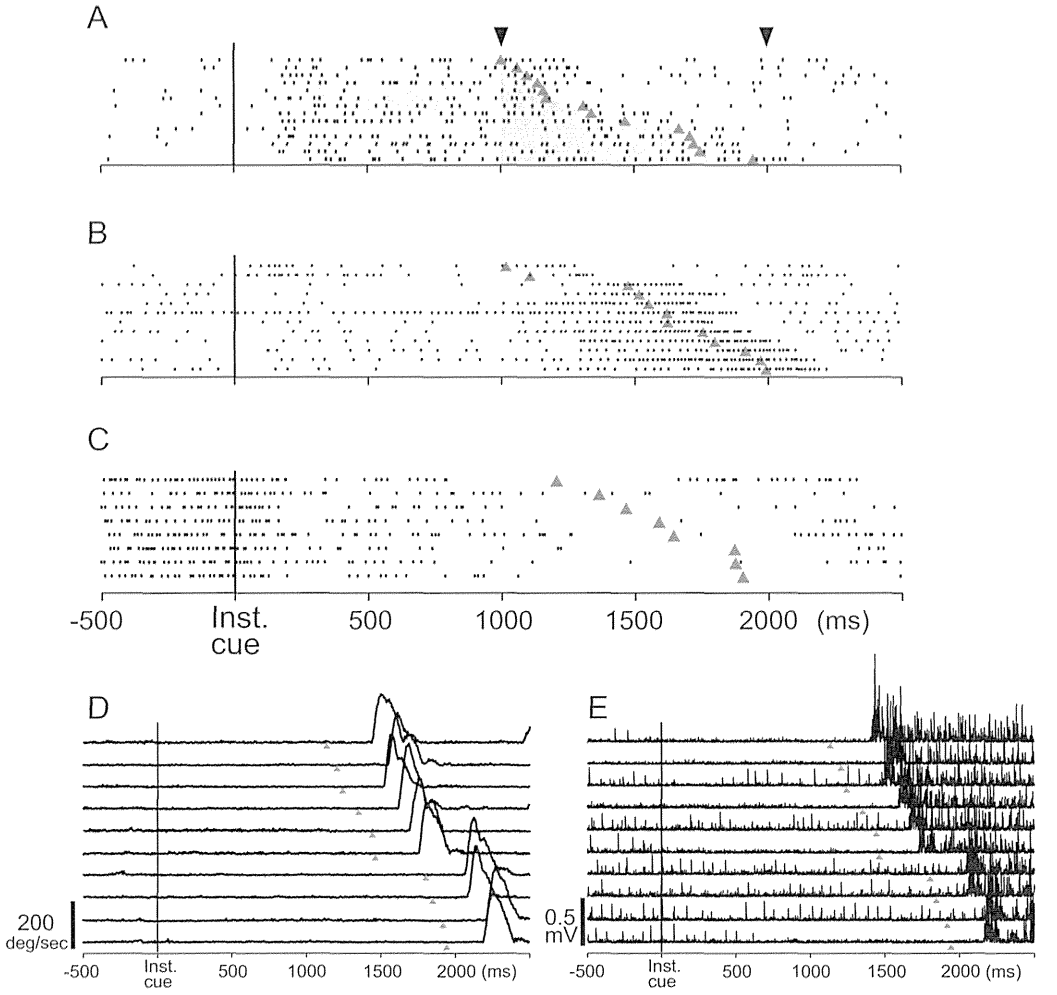


**Fig. 1.** Three representative types of delay activity in MFs during delay period. (A–C) Raster plots are aligned on the time of instruction cue presentation. Plots for individual trials are sorted by the duration of delay period from top to bottom. (A) MF with an increase in activity triggered by instruction cue presentation in a representative movement direction. The activity change started in the early delay period (0–1000 ms after instruction cue presentation). Black filled triangles above the raster plots indicate the possible timing of the earliest and the latest go signal. Averaged firing rates in the blue shaded area of 'early delay period' (from 300 to 800 ms after instruction cue presentation) and the red shaded area (the 'late delay period' starting at 1000 ms after instruction cue) were used to calculate the significance of activity change in each delay period. Red triangles indicate the timing of the go signal. (B) MF with increase in activity in the late delay period (more than 1000 ms after instruction cue presentation). (C) MF with decrease in activity during the early and late delay periods. Velocity of the wrist movement (D) and electromyogram of the extensor carpi ulnaris (E) recorded simultaneously for movements to down right, which showed the largest movement-related activity of the muscle. Both velocity and EMG activity showed little change before the go signal. (For interpretation of the references to color in this figure legend, the reader is referred to the web version of the article.)

to represent an excitatory postsynaptic potential in granule cells (Walsh et al., 1974), it is highly likely that we recorded the MF spikes near glomeruli. After recording unit activities, we examined the peripheral receptive fields (RFs) of recorded MFs. We used passive movements and palpation or brushing of the fingers, forearm, upper arm, shoulder, neck, chest, abdomen, back, face, and leg on both sides of the body to search for somatosensory afferent input. We estimated the location of the primary fissure from an MRI image and made recordings mainly from lobules V to VI, where granule cells receive projections from the arm area of M1 (Kelly and Strick, 2003) via MFs. All animal experimentation was conducted in accordance with the Guide for the Care and Use of Laboratory Animals (National Research Council, Washington, DC: National Academy Press, 1996) and the Guiding Principles for the Care and Use of Animals in the Field of Physiological Sciences (The Physiological Society of Japan, revised 2001). All surgical and experimental protocols were approved by the Animal Care and Use Committee of Tokyo Metropolitan Institute of Medical Science, and all efforts were made to minimize suffering.

We recorded 230 MFs showing clear and reproducible modulation of activity during the task (150 and 80 from monkeys M and S). In order to exclude MFs that may not be directly linked to wrist movement, we eliminated MFs with RFs outside the ipsilateral forearm. Thus, this study included 155 task-related MFs (105 and 50 from monkeys M and S). All 155 MFs showed modulation of activity between instruction cue presentation and go signal and/or phasic activity at movement onset. Because the go signal did not appear during the initial 1000 ms of the instruction period, we used 1000 ms after instruction cue presentation as a boundary to separate the delay period into two time windows. We defined the time period 1000 ms from instruction cue presentation as the 'early delay period' and the remaining delay period before the go signal as the 'late delay period'. Therefore, the duration of the late delay period ranged from 0 to 1000 ms and varied from trial to trial. We looked for significant changes in modulation during the delay periods by comparing the mean ± 2SD of averaged firing rate during the 500 ms (10 bins of 50 ms width) before instruction cue presentation with the mean firing rates in the early and late delay periods (blue and red shaded areas in Fig. 1A). Because the late delay period

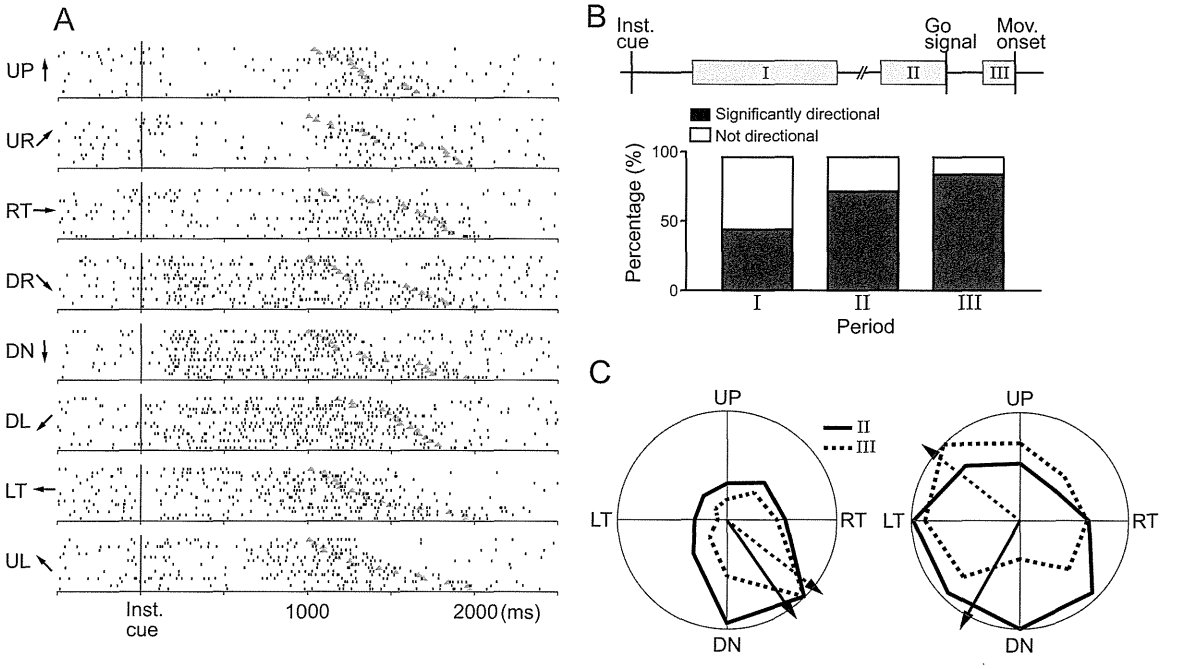


**Fig. 2.** Directional tuning of representative MF activity during the delay period. (A) Raster plots of directionally-tuned MF activity in eight directions. Red triangles indicate the timing of go signal. UP: upward, RT: right, DN: downward, LT: left. UP, DN, LF and RT correspond to extension, flexion, radial deviation and ulnar deviation of the wrist joint, respectively. (B) Percentage of MFs showing directionally tuned activity in three time windows, indicated as I–III. I: 300–800 ms after Instruction cue presentation. II: 1000 ms after Instruction cue to go signal. III: −100 to 0 ms before movement onset. Percentages were 45.7, 81.4 and 87.1 in periods I, II and III, respectively. Averaged firing rate in each time window was calculated in eight directions and the significance of directionality was examined using a Rayleigh test. (C) Polar plots of activity during time windows II (solid line) and III (dotted line) in two MFs. Arrows indicate PD of the activity in each time window. Left panel shows an example of MF activity that did not show a change in PD. Right panel shows an example of MF activity that showed a significant change of PD between the two time periods. (For interpretation of the references to color in this figure legend, the reader is referred to the web version of the article.)

varied in duration, the mean firing rate in the late delay period was calculated by dividing total number of spikes by total duration of the late delay period.

We found that 70 MFs (49 and 21 from monkeys M and S) among the 155 task-related MFs (45%) showed a significant increase or decrease of activity during the delay period for one or more movement directions. It should be noted that MFs often showed different patterns of modulation, depending on movement direction. Forty-six of 70 MFs showed an increase in the early delay period (Fig. 1A), and 68/70 MFs showed an increase in the late delay period (Fig. 1B) in at least one movement direction. On the other hand, 47/70 MFs showed significant suppression of activity in one or both delay periods (Fig. 1C). Onset and/or offset of the suppressions were often unclear because of low firing rate and gradual modulation change. Modulation changes that started in the early delay period either decayed in the late delay period or continued beyond the go signal. Modulation changes that started in the late delay period were sustained beyond the go signal. No MFs showed phasic activity characterized as a visual response to cue presentation. During the delay period, cursor position remained stable, as shown by the lack of change in velocity and muscle activity (Fig. 1D and E).

The different patterns of delay activity among the eight movement directions in individual MFs resulted mainly from directional tuning of the activity. As an example, the MF illustrated in Fig. 2A showed a significant increase of activity in three directions (DR, DN, and DL), with no significant modulation in other directions, during the early delay period. This pattern derived from significant directional tuning (Rayleigh test, $p = 0.05$) of the MF activity. Other directionally-tuned MF activity contained both increases and decreases or only decreases of activity among the eight directions. Overall, 32 and 57 MFs showed significant directionality in the early and late delay periods, respectively (Fig. 2B). The number of MFs showing directional tuning rose further around movement onset ($n = 61$, Fig. 2B). In each period, the distribution of preferred directions (PDs) was not significantly biased (Rayleigh test, $p = 0.05$). Twenty-seven MFs showed directional tuning in both delay periods, and the PD of the activity for 25/27 MFs remained within the 95% confidence interval during both periods (bootstrapping test, 10,000 repetitions). In addition, 48 MFs showed directional tuning in both the late delay period and right before movement onset. Most of these ($n = 41/48$) did not show a significant change of PD between periods (Fig. 2C left). Only seven MFs had a significant change of PD between late delay and movement periods (Fig. 2C right). Overall, PDs remained constant throughout the task for most MFs. A few MFs ($n = 3$) had uniform modulation in all directions and consequently were non-directional.

Most MFs ($n = 55/70$, ~80%) showed a relationship between the duration of the delay period and their delay activity (Fig. 3A). That is, we observed a significant correlation between the duration of the late delay period and spike frequency in the last 200 ms of the delay period in one or more directions (Fig. 3B, Pearson's correlation coefficient, $p = 0.05$). The correlation was either positive or negative, independent of movement direction, for most of these MFs (51/55). Considering that a longer delay period resulted in a larger modulation change and vice versa, this result may suggest that the MF activity right before the go signal is involved in either predicting or preparing for an upcoming event. However, we did not observe a modulation change right before instruction cue presentation, even though the instruction cue also was predictable. This makes it unlikely that the late delay activity is predicting the timing of the go signal. Rather, we interpret the late delay activity of MFs as a motor preparatory signal in anticipation of the upcoming go signal.

All MFs with delay activity also showed a modulation change around movement onset in one or more directions (Fig. 3C). The activity pattern (onset/offset, duration and size of modulation)

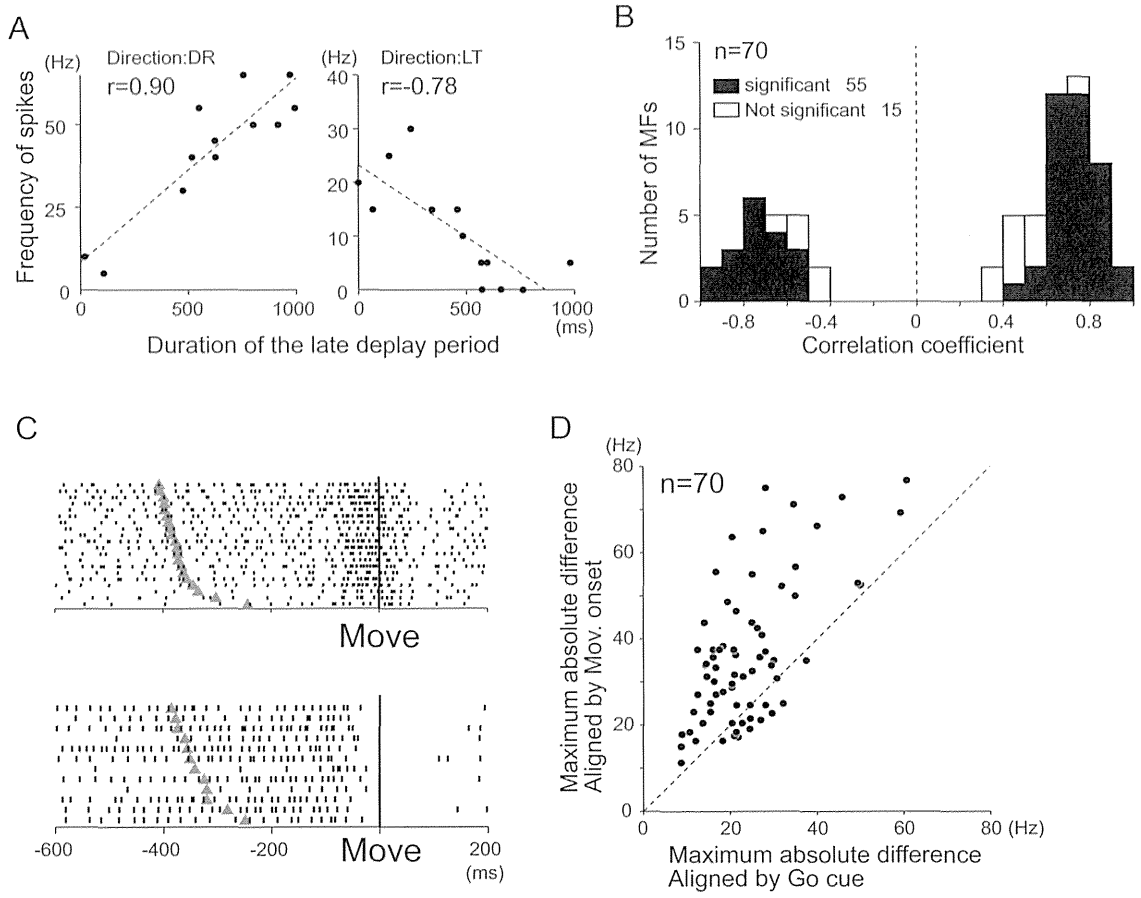


**Fig. 3.** Change of MF activity before and after go signal. (A) A representative MF that showed a high correlation between the duration of the late delay period and frequency of spikes in the last 200 ms of the delay period. The regression line is shown. Left plot shows a positive correlation for down-right movements and right plot shows a negative correlation for leftward movements. (B) Histogram of the highest correlation coefficient for each MF. Filled squares indicate MFs with significant ($p < 0.05$) correlations. (C) Representative activity patterns of a MF aligned on movement onset. Raster plots of each trial were sorted by reaction time from top to bottom. Red triangles indicate the timing of the go signal. MFs showed either a burst or pause that started before or after movement onset. Both types of activity were observed in individual MFs. (D) Scatter plot showing instantaneous change of firing rate calculated from data aligned on the go signal vs. data aligned on movement onset. For this analysis, we used histograms of firing rate in 40 ms bins for each alignment. Then, we calculated the difference in firing rate between neighboring bins for each alignment. The scatter plot shows the largest change in firing rate in the go signal-aligned vs. the movement onset-aligned data for each MF. This analysis demonstrates that the activity change was time-locked to movement onset. (For interpretation of the references to color in this figure legend, the reader is referred to the web version of the article.)

depended on movement direction. Onset or offset of the modulation was time-locked to movement onset rather than to the go signal (Fig. 3D, *t*-test, $p = 0.01$), even though the modulation started before the go signal. Therefore, the prolonged change of activity beyond the go signal is likely related to movement execution.

The MFs showing delay activity reported in this study had clear somatosensory RFs in the ipsilateral forearm and/or hand and fingers, although a few MFs did not respond to somatosensory stimulation. In both monkeys, the MFs were distributed as a large cluster over lobules V and VI and overlapped MFs with RFs in the proximal part of the arm. MFs with RFs in the leg and orofacial area were distributed rostrally and caudally (Fig. 4A). Thus, the MFs displayed a rostro-caudal arrangement of leg, forelimb and orofacial regions and matched the generally-accepted somatotopy of the cerebellar cortex (Adrian, 1943). The distributions of MFs with and without delay activity did not differ (Fig. 4B).

This is the first report of MFs showing prolonged activity in a delay period before movement execution. Those MFs were widely distributed in the cerebellar hemisphere where major afferent inputs derive from M1 and PM (Kelly and Strick, 2003; Lu et al., 2007; Hashimoto et al., 2010). In our previous studies, we reported that neurons in ventral PM and M1 demonstrated modulation of activity during the delay period in the same task conditions (Kakei et al., 1999, 2001). Therefore, the delay activity in MFs may originate from PM and M1. Indeed, we found that there were common features in the delay activity of M1/PM neurons and the MFs. First, as observed in PM and M1 (Tanji and Evarts, 1976; Weinrich and Wise, 1982; Kurata and Wise, 1988; Crammond and Kalaska, 1994; Nakayama et al., 2008; Kurata, 2010), most MFs had delay activity triggered by instruction cue presentation. Second, many MFs showed modulation changes that started more than 1000 ms after instruction cue presentation, i.e., after the earliest timing of go signal. Similar anticipatory activity was observed after the earliest timing of the go signal in PM neurons in previous studies (Fig. 13 in Weinrich et al., 1984; Fig. 3C in Kurata, 2010). Third, prolonged delay period activity beyond the go signal was significantly modulated in relation to movement execution, similar to that in PM and M1 (Crammond and Kalaska, 2000). Fourth, the activities of most MFs showed directional tuning, as observed in M1/PM neurons in the same task condition (Kakei et al., 1999, 2001). Overall, we found that the patterns of delay activity in PM and/or M1 were surprisingly well-preserved in the recorded MF activity. Though we have no direct evidence that the MFs described here originated from the cortical motor areas, the delay activity could not be evoked if the MFs originated from spinal cord. As shown in Fig. 1D and E, there was little or no change in movement kinematics and muscle activity during the delay period. Therefore, we concluded that the recorded delay activity of MFs was cortico-ponto-cerebellar

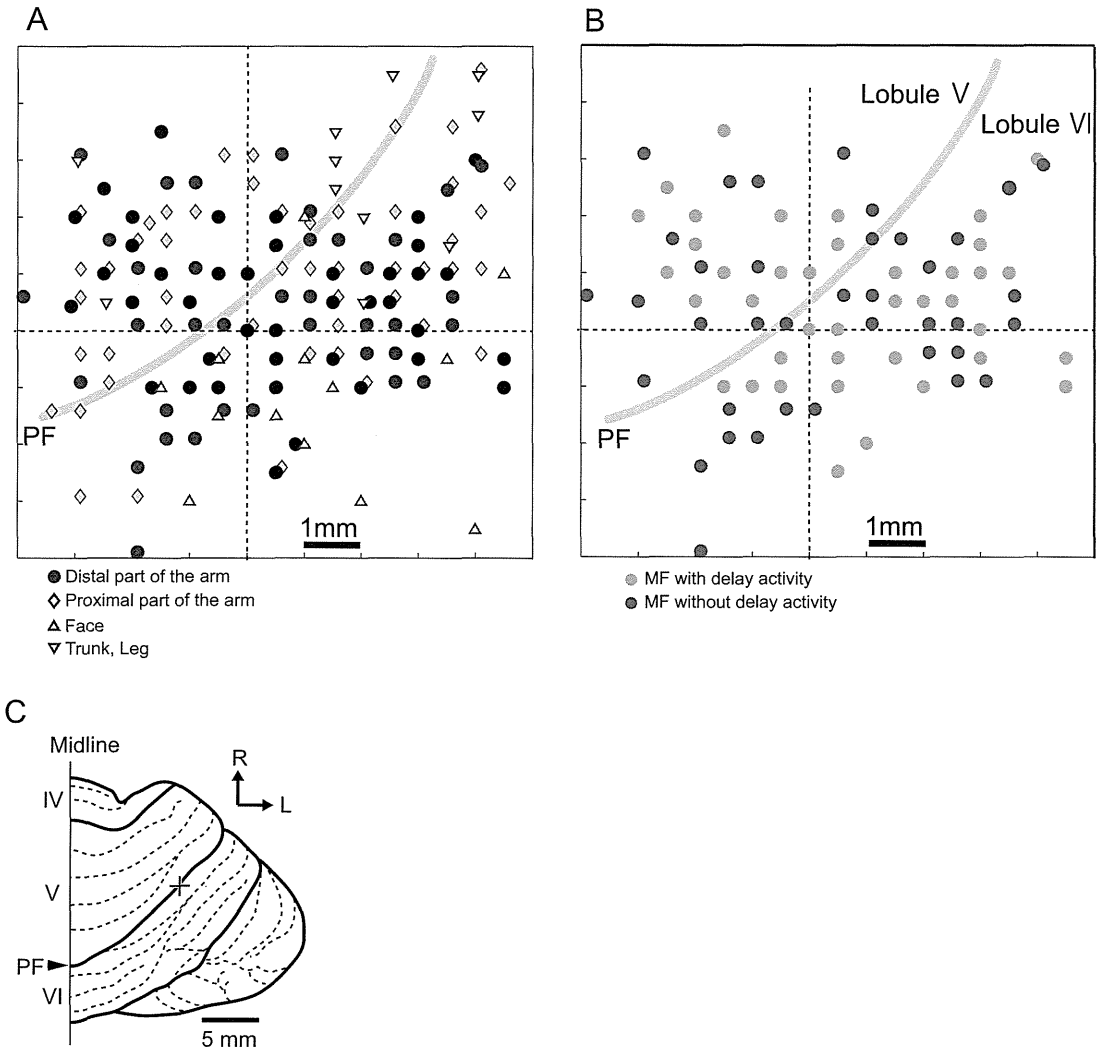


**Fig. 4.** Distribution of recorded MFs. (A) Somatotopy map of MFs in monkey M. Symbols indicate MFs with RFs in distal part of the ipsilateral arm (●), proximal part of the ipsilateral arm (◇), orofacial area (△), trunk and leg (▽). Gray line indicates putative location of the primary fissure. (B) Map of MFs with delay activity (blue dots) and without delay activity (red dots) in monkey M. Similar maps were obtained from monkey S. (C) Dorsal view of the cerebellar hemisphere and the center of the recording chamber (+) estimated from MRI image in monkey M. (For interpretation of the references to color in this figure legend, the reader is referred to the web version of the article.)

input that likely originated from M1 and PM. Considering the intensive divergence and convergence of the cortico-pontine projection (Schwarz and Thier, 1995; Bjaalie et al., 1997; Brodal and Bjaalie, 1997), it was assumed that the original spatio-temporal patterns of cortical inputs would be transformed to generate integrated representations in the PN. Nevertheless, we found that delay activities of MFs basically resembled activities of PM or M1 neurons (Kakei et al., 1999, 2001), and furthermore, somatosensory RFs of the MFs were rather localized. These observations suggest that each PN neuron receives inputs from a limited number of motor cortical neurons that have similar activity patterns and maintain their RFs.

M1 and PM project to the cerebellum via PN, and the dentate nucleus (DN), the output channel of the hemispheric part of the cerebellum, sends output to the motor cortices via motor thalamus. In the cerebro-cerebellar loop, delay period activities were observed in M1/PM (Tanji and Evarts, 1976; Weinrich and Wise, 1982; Kurata and Wise, 1988; Crammond and Kalaska, 1994; Kakei et al., 1999, 2001; Nakayama et al., 2008; Kurata, 2010), in putative PN (as MFs, present study) and in the motor thalamus (Kurata, 2005) during an arm movement task. We also observed delay activity of DN neurons in the same task used here (unpublished observations). The delay period activity in DN is compatible with a recent report by Ashmore and Sommer (2013), which demonstrated delay activity of saccade-related neurons in caudal DN. These findings suggest that the concomitant delay activities along the whole cerebro-cerebellar loop may play an important role for planning and/or preparation for upcoming movement. Indeed, dysfunction of the cerebellum caused by ablation or cooling resulted in a delay in the activation of M1 neurons and in the onset of EMG activity and movement (Meyer-Lohmann et al., 1977; Sasaki et al., 1981) during a limb movement task in monkeys. Impaired cerebellar activity may prevent the development of delay activity that facilitates prompt activation of M1/PM neurons and smooth initiation of movement. Examination of this hypothesis is one of the important challenges for our future studies.

## Acknowledgements

This work was supported by the Tokyo Metropolitan Institute of Medical Science and grants-in-aid from the Japan Science and Technology Agency (PRESTO: Intelligent Cooperation and Control) and from KAKENHI to T.I. (No. 24650224), S.K. (Nos. 14580784, 15016008, 16015212, 20033029, and 21500319), and S.T. (Nos. 18700492 and 20700478).

## References


Adrian, E.D., 1943. Afferent area in the cerebellum connected with the limbs. Brain 66, 289–315.

Ashmore, R.C., Sommer, M.A., 2013. Delay activity of saccade-related neurons in the caudal dentate nucleus of the macaque cerebellum. J. Neurophysiol. 109, 2129–2144.

Bjaalie, J.G., Sudbo, J., Brodal, P., 1997. Corticopontine terminal fibres form small scale clusters and large scale lamellae in the cat. Neuroreport 8, 1651–1655.

Bourbonnais, D., Krieger, C., Smith, A.M., 1986. Cerebellar cortical activity during stretch of antagonist muscles. Can. J. Physiol. Pharmacol. 64, 1202–1213.

Brodal, P., Bjaalie, J.G., 1997. Salient anatomic features of the cortico-ponto-cerebellar pathway. Prog. Brain Res. 114, 227–249.

Crammond, D.J., Kalaska, J.F., 1994. Modulation of preparatory neuronal activity in dorsal premotor cortex due to stimulus–response compatibility. J. Neurophysiol. 71, 1281–1284.

Crammond, D.J., Kalaska, J.F., 2000. Prior information in motor and premotor cortex: activity during the delay period and effect on pre-movement activity. J. Neurophysiol. 84, 986–1005.

Hashimoto, M., Takahara, D., Hirata, Y., Inoue, K., Miyachi, S., Nambu, A., Tanji, J., Takada, M., Hoshi, E., 2010. Motor and non-motor projections from the cerebellum to rostrocaudally distinct sectors of the dorsal premotor cortex in macaques. Eur. J. Neurosci. 31, 1402–1413.

Hoshi, E., Tanji, J., 2002. Contrasting neuronal activity in the dorsal and ventral premotor areas during preparation to reach. J. Neurophysiol. 87, 1123–1128.

Kakei, S., Hoffman, D.S., Strick, P.L., 1999. Muscle and movement representations in the primary motor cortex. Science 285, 2136–2139.

Kakei, S., Hoffman, D.S., Strick, P.L., 2001. Direction of action is represented in the ventral premotor cortex. Nat. Neurosci. 4, 1020–1025.

Kelly, R.M., Strick, P.L., 2003. Cerebellar loops with motor cortex and prefrontal cortex of a nonhuman primate. J. Neurosci. 23, 8432–8444.

Kurata, K., 2005. Activity properties and location of neurons in the motor thalamus that project to the cortical motor areas in monkeys. J. Neurophysiol. 94, 550–566.

Kurata, K., 2010. Conditional selection of contra- and ipsilateral forelimb movements by the dorsal premotor cortex in monkeys. J. Neurophysiol. 103, 262–277.

Kurata, K., Wise, S.P., 1988. Premotor cortex of rhesus monkeys: set-related activity during two conditional motor tasks. Exp. Brain Res. 69, 327–343.

Lu, X., Miyachi, S., Ito, Y., Nambu, A., Takada, M., 2007. Topographic distribution of output neurons in cerebellar nuclei and cortex to somatotopic map of primary motor cortex. Eur. J. Neurosci. 25, 2374–2382.

Meyer-Lohmann, J., Hore, J., Brooks, V.B., 1977. Cerebellar participation in generation of prompt arm movements. J. Neurophysiol. 40, 1038–1050.

Nakayama, Y., Yamagata, T., Tanji, J., Hoshi, E., 2008. Transformation of a virtual action plan into a motor plan in the premotor cortex. J. Neurosci. 28, 10287–10297.

Sasaki, K., Gemba, H., Hashimoto, S., 1981. Influences of cerebellar hemispherectomy upon cortical potentials preceding visually initiated hand movements in the monkey. Brain Res. 205, 425–430.

Schwarz, C., Thier, P., 1995. Modular organization of the pontine nuclei: dendritic fields of identified pontine projection neurons in the rat respect the borders of cortical afferent fields. J. Neurosci. 15, 3475–3489.

Tanji, J., Evarts, E.V., 1976. Anticipatory activity of motor cortex neurons in relation to direction of an intended movement. J. Neurophysiol. 39, 1062–1068.

Taylor, A., Elias, S.A., Somjen, G., 1987. Focal synaptic potentials due to discrete mossy-fibre arrival volleys in the cerebellar cortex. Proc. R. Soc. Lond. B: Biol. Sci. 231, 217–230.

van Kan, P.L., Gibson, A.R., Houk, J.C., 1993. Movement-related inputs to intermediate cerebellum of the monkey. J. Neurophysiol. 69, 74–94.

Walsh, J.V., Houk, J.C., Mugnaini, E., 1974. Identification of unitary potentials in turtle cerebellum and correlations with structures in granular layer. J. Neurophysiol. 37, 30–47.

Weinrich, M., Wise, S.P., 1982. The premotor cortex of the monkey. J. Neurosci. 2, 1329–1345.

Weinrich, M., Wise, S.P., Mauritz, K.H., 1984. A neurophysiological study of the premotor cortex in the rhesus monkey. Brain 107, 385–414.

Cerebellum
DOI 10.1007/s12311-013-0514-7

REVIEW

# Non-invasive Cerebellar Stimulation—a Consensus Paper

**G. Grimaldi · G. P. Argyropoulos · A. Boehringer · P. Celnik · M. J. Edwards · R. Ferrucci · J. M. Galea · S. J. Groiss · K. Hiraoka · P. Kassavetis · E. Lesage · M. Manto · R. C. Miall · A. Priori · A. Sadnicka · Y. Ugawa · U. Ziemann**



**Abstract** The field of neurostimulation of the cerebellum either with transcranial magnetic stimulation (TMS; single pulse or repetitive (rTMS)) or transcranial direct current stimulation (tDCS; anodal or cathodal) is gaining popularity in the scientific community, in particular because these stimulation techniques are non-invasive and provide novel information on cerebellar functions. There is a consensus amongst the panel of experts that both TMS and tDCS can effectively influence cerebellar functions, not only in the motor domain, with effects on visually guided tracking tasks, motor surround inhibition, motor adaptation and learning, but also for the cognitive and affective operations handled by the cerebro-cerebellar circuits. Verbal working memory, semantic associations and predictive language processing are amongst these operations. Both TMS and tDCS modulate the connectivity between the cerebellum and the primary motor cortex, tuning cerebellar excitability. Cerebellar TMS is an effective and valuable method to evaluate the cerebello-thalamo-cortical

G. Grimaldi (✉) · M. Manto
Unité d'Etude du Mouvement, Hôpital Erasme-ULB, 808 Route de Lennik, 1070 Brussels, Belgium
e-mail: giulianagrim@yahoo.it

G. P. Argyropoulos
Department of Psychology, Brain, Action and Cognition Lab, Royal Holloway, University of London, Wolfson Building, Egham, Surrey TW20 0EX, UK

A. Boehringer
Department of Neurology, Max Planck Institute for Human Cognitive and Brain Sciences, Leipzig, Germany

A. Boehringer
Central Institute for Mental Health, Mannheim, Germany

P. Celnik
Johns Hopkins University Baltimore, Baltimore, MD, USA

M. J. Edwards · P. Kassavetis · A. Sadnicka
Sobell Department of Motor Neuroscience and Movement Disorders, UCL Institute of Neurology, Queen Square, London WC1N 3BG, UK

R. Ferrucci · A. Priori
Centro Clinico per la Neurostimolazione, le Neurotecnologie ed i Disordini del Movimento Fondazione IRCCS Cà Granda, Ospedale Maggiore Policlinico, Milan, Italy

R. Ferrucci · A. Priori
Dipartimento di Fisiopatologia Medico-Chirurgica e dei Trapianti, Università degli Studi di Milano, Milan, Italy

J. M. Galea
School of Psychology, University of Birmingham, Birmingham, UK

S. J. Groiss
Centre for Movement Disorders and Neuromodulation, Department of Neurology and Institute for Clinical Neuroscience and Medical Psychology, Medical Faculty, Heinrich-Heine-University, Düsseldorf, Germany

K. Hiraoka
School of Comprehensive Rehabilitation, Osaka Prefecture University, 3-7-30 Habikino, Habikino, Osaka 583-8555, Japan

E. Lesage · R. C. Miall
School of Psychology, University of Birmingham, Birmingham, UK

M. Manto
FNRS, Brussels, Belgium

Y. Ugawa
Department of Neurology, School of Medicine, Fukushima Medical University, Fukushima, Japan

U. Ziemann
Department of Neurology and Stroke, Hertie-Institute for Clinical Brain Research, Eberhard Karls University, Tübingen, Germany

Published online: 14 August 2013

loop functions and for the study of the pathophysiology of ataxia. In most circumstances, DCS induces a polarity-dependent site-specific modulation of cerebellar activity. Paired associative stimulation of the cerebello-dentato-thalamo-M1 pathway can induce bidirectional long-term spike-timing-dependent plasticity-like changes of corticospinal excitability. However, the panel of experts considers that several important issues still remain unresolved and require further research. In particular, the role of TMS in promoting cerebellar plasticity is not established. Moreover, the exact positioning of electrode stimulation and the duration of the after effects of tDCS remain unclear. Future studies are required to better define how DCS over particular regions of the cerebellum affects individual cerebellar symptoms, given the topographical organization of cerebellar symptoms. The long-term neural consequences of non-invasive cerebellar modulation are also unclear. Although there is an agreement that the clinical applications in cerebellar disorders are likely numerous, it is emphasized that rigorous large-scale clinical trials are missing. Further studies should be encouraged to better clarify the role of using non-invasive neurostimulation techniques over the cerebellum in motor, cognitive and psychiatric rehabilitation strategies.

**Keywords** Cerebellum · Transcranial magnetic stimulation · Direct current stimulation · Anodal · Cathodal · Motor adaptation · Excitability · Cerebellar inhibition · Paired associative stimulation · Vision · Language · Predictions · Motor surround inhibition · Working memory · Semantic associations · Ataxia

**Abbreviations**

| | |
|---|---|
| ADM | Abductor digiti minimi |
| BCIs | Brain–computer interfaces |
| CB | Cerebellum |
| CBI | Cerebellar–brain inhibition |
| cSP | Cortical silent period |
| cTBS | Continuous theta burst stimulation |
| DCS | Direct current stimulation |
| EMG | Electromyographic |
| FDI | First dorsal interosseous |
| fMRI | Functional magnetic resonance imaging |
| LICI | Long interval intracortical inhibition |
| LTD | Long-term depression |
| LTP | Long-term potentiation |
| M1 | Primary motor cortex |
| MEP | Motor evoked potential |
| mSI | Motor surround inhibition |
| PAS | Paired associative stimulation |
| PET | Positron emission tomography |
| PSP | Progressive supranuclear palsy |
| rTMS | Repetitive transcranial magnetic stimulation |
| SICI | Short interval intracortical inhibition |
| SRTT | Serial reaction time task |
| STDP | Spike-timing-dependent plasticity |
| tDCS | Transcranial direct current stimulation |
| TES | Transcranial electric stimulation |
| TMS | Transcranial magnetic stimulation single shock |
| VAS | Visual analogue scale |
| VWM | Verbal working memory |

## Introduction

Non-invasive cerebellar neuromodulation has recently increased its attractiveness in both the neuroscience and neurorehabilitation communities. This consensus paper aims to present current views on transcranial magnetic stimulation (TMS) and transcranial direct current stimulation (tDCS; anodal or cathodal) in studies devoted to cerebellar functions, not only for a better understanding of the roles of the cerebellar circuitry in the central nervous system but also for a potential neuromodulation in the motor domain and in the neurocognitive field. Indeed, the cytoarchitectural homogeneity of the cerebellum and its closed parallel loop-like connectivity with cerebrocortical areas are striking features [1, 2], leading to the idea that the cerebellum performs similar operations on the numerous input signals that it receives. Evidence from clinical and neuroimaging studies that the cerebellum contributes to cognition will not be developed in the present report. The reader is referred to the article of Stoodley and Schmahmann for a review on this topic [1].

The panel of experts provides lines of consensus and identifies unclear points requiring further studies. The following specific topics will be covered: the roles of TMS to elucidate cerebellar functions, the mechanisms underlying the dynamic modulation of cerebellar excitability, the potential applications of tDCS of the cerebellum in cerebellar ataxias, paired associative stimulation of human cerebellum and primary motor cortex, visually guided tracking tasks, motor surround inhibition, motor adaptation, the modulation of learning by cerebellar tDCS, the contribution of cerebellum in verbal working memory and in semantic associations, the role of rTMS to investigate predictive language processing.

## Cerebellar Neurostimulation. What Have We Learnt from TMS Studies?

The cerebellum is well known to play important roles in movement execution and motor control by modulation of the primary motor cortex (M1) through cerebello-thalamo-cortical connections [3]. The cerebellum receives inputs from the cortex mainly through the middle cerebellar peduncle in